Chapter 3
Rheological and Thickening Properties

Katsuyoshi Nishinari

Abstract Rheology in food studies all the mechanical properties relating deformation and flow. Since the texture is known to be important to govern the palatability with taste and aroma, and also recognized as a key factor in designing foods for persons with difficulty in mastication and deglutition, hydrocolloids controlling rheological and thickening properties have been attracting more attention than before. This chapter describes the necessity and importance of rheology and then, fundamental concept of elasticity, viscosity, static and dynamic viscoelasticity, and the measuring methods in relation with the molecular structure. Although yield stress and thixotropy have been recognized and studied, they are both not so well understood, and recent developments are described in relation with thickening properties. Recent development of fractional calculus and microrheology is described. Application of thickening properties is also described.

Keywords Viscosity · Elasticity · Viscoelasticity · Yield stress · Thixotropy

1 Introduction

Rheology is a science on the deformation and flow of matters. The word rheology is the combination of "rheo"—flow and "logy"—science in Greek. In the early stage of rheology, British Rheologists Club (1942) proposed a classification of deformation which is divided into elastic deformation and flow. Between the two most simple extremities, Hookean elasticity and Newtonian viscosity, viscoelastic deformation has been most well studied in relation with plastic industry and food industry. Rheology has been proved to be useful to understand quantitatively the gelation process (treated in the next chapter), the transformation of a liquid to solid, dispersed systems, the mixture of different materials because most foods consist of many

K. Nishinari (✉)
Glyn O. Phillips Hydrocolloids Research Centre, School of Food and Biological Engineering, Hubei University of Technology, Wuhan, PR China
e-mail: katsuyoshi.nishinari@hbut.edu.cn

Y. Fang et al. (eds.), *Food Hydrocolloids*,
https://doi.org/10.1007/978-981-16-0320-4_3

ingredients. Rheology is developing steadily influenced by the development of other related science. The new measurement techniques such as atomic force microscopy, optical tweezers in microrheology make possible to detect the nano/micro scale distance, and the length scale studied in rheology is widened to nano, micro, meso, and macroscale. Femtosecond spectroscopy and time-resolved X-ray diffraction photoelectron spectroscopy study the very fast change of rheological properties accompanying the structural changes, and the timescale is also widened. Rheology is also closely related with dielectric (e.g. broadband dielectric measurement) and related studies, and thus can be treated from the common background such as stimulus-response theory. Stimulus-response approach has been proved useful to understand systematically the transient phenomena in statistical physics, but now it seems to be used also in psychology. Remember the conditioned reflexes of Pavlov's dog. It is expected to be applied to sensory evaluation of texture and flavor of foods. Soft matters such as foods, biological tissues, polymers, colloids are now understood based on common background (de Gennes 1979; Doi 2013). Rheology in food has been studied extensively because the perceived texture is closely correlated with rheology (Bourne 2002; Chen and Engelen 2012; Nishinari and Fang 2018). As is widely recognized, texture and flavor are most important attributes governing the palatability of foods. With the advent of aged society, the number of persons who have the difficulty in the mastication and swallowing is increasing, which increases the number of cases of pneumonia and other symptoms. Rheology is not yet completed for food science, and more developments are expected to solve these problems and to create better foods, better storage, and distribution methods in collaboration with other disciplines. It is widely recognized that instrumental measurements give the objective evaluation and basis of the perceived texture of foods which are described by subjective terms. Interpretation of sensory terms such as firm, hard, stiff, rigid, etc. is often confusing and depends on individuals.

Although the elastic modulus obtained from the initial slope of force-deformation curves of the agar gel is larger than that of the gelatin gel (Fig. 3.1a), the breaking strength of the agar gel turns out to be smaller than that of the gelatin gel even after the calibration of the cross-sectional area. Therefore, it is impossible to answer to a question "which of the two gels, an agar gel or a gelatin gel, is 'firmer' or 'harder'?" if the definition of the hardness or the firmness is not given.

In Fig. 3.1b, how we could answer to the question "Which of the two liquids, sugar syrup or mayonnaise, is thicker?" Most people reply that sugar syrup is thicker than mayonnaise. This indicates that most people sense the viscosity at a higher shear rate than ca. 1 s^{-1} in the mouth. As shown in this example, daily language such as "thick" and "thin" is vague.

Scott Blair studied the relation between the instrumental measurement and sensory evaluation of texture using fractional calculus which has recently re-attracted more attention. Although the theory of viscoelasticity is well developed in the linear region where the stress and strain or strain rate are in the linear relation, the large deformation and fracture are not so well established. In this chapter, after describing the basic concepts in the linear viscoelasticity, large amplitude oscillatory shear (LAOS), yield stress, thixotropy, microrheology are described. Application of thickening agents in food production is also described. Then, recent application of

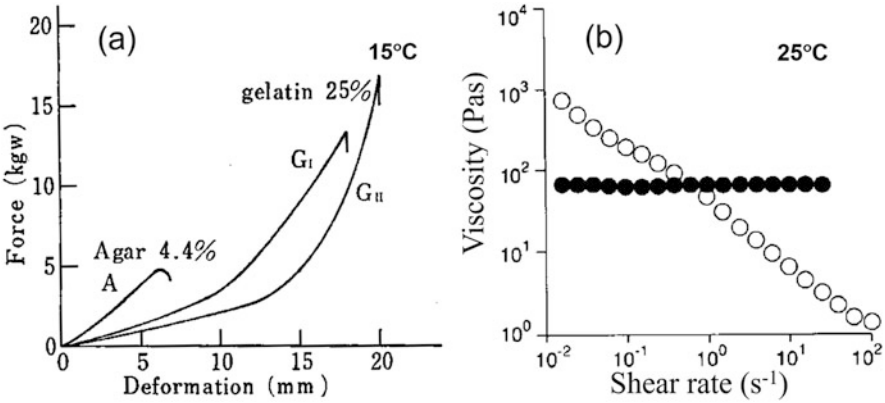

Fig. 3.1 (**a**) Force-deformation curves of cylindrical (20 mm diameter and 30mm height) gels of 4% agar and 25% gelatin at a compression velocity of 10 mm/min. The curve G_I and G_{II} for gelatin gels were obtained with approximately equal probability (Nishinari et al. 1980). (**b**) The viscosity as a function of shear rate for sugar syrup (closed circle, flow behavior similar to honey) and mayonnaise (open circle). Reproduction with permission from Nishinari et al. (1980). Copyright 1980 JSFST

fractional calculus and also the relation between the molecular structure and viscosifying function are described.

2 Elasticity

Theory of elasticity treats the deformation of solids. Solids do not flow and maintain a certain shape. A solid which does not deform at all even under a force is called a "rigid body." The distance between two points in a rigid body is regarded as constant. The concept of a rigid body is an ideal model. In reality, even a diamond or iron deforms when it is subjected to a large force.

The simplest model of a deformable solid is an elastic body. An elastic body shows a constant strain (ratio of deformation) instantaneously, that is without delay, when it is subjected to a constant stress (force per unit area). This solid is called a Hookean body. Imagine a rod of a radius r and a length l which is subjected to a force f. Hooke's law for this rod is written as $f/(\pi r^2) = E\,(\delta l/l)$, where the left-hand side is the force per unit area, which is called (elongational or compressional) stress, while the right-hand side is the product of the elastic constant E and the (elongational or compressional) strain. Elongational strain indicates the ratio of the deformation δl to the initial length l, and it is often written as $\varepsilon = \delta l/l$. Elastic constant E defined for the elongational or compressional deformation is called Young's modulus, which represents the stress required to produce the unit elongation or unit contraction. It indicates the resistance to the deformation. The unit of E is force over area, that is Pa = N/m^2, in SI.

When the force f is exerted on the upper surface of the parallelepiped body to the parallel direction of the surface, then it shows a uniform deformation which is

Table 3.1 The relation between 4 elastic parameters

	G,E	G, κ	E, κ	G, μ	E, μ	κ, μ
G	G	G	$\frac{3\kappa E}{9\kappa - E}$	G	$\frac{E}{2(1+\mu)}$	$\frac{3\kappa(1-2\mu)}{2(1+\mu)}$
E	E	$\frac{9G\kappa}{G+3\kappa}$	E	$2(1+\mu)G$	E	$3\kappa(1-2\mu)$
κ	$\frac{GE}{9G-3E}$	κ	κ	$\frac{2(1+\mu)G}{3(1-2\mu)}$	$\frac{E}{3(1-2\mu)}$	κ
μ	$\frac{E-2G}{2G}$	$\frac{3\kappa-2G}{2(3\kappa+G)}$	$\frac{3\kappa-E}{6\kappa}$	μ	μ	μ

characterized by a small angle γ. For a small angle, $\tan\gamma$ can be approximated by γ, which is called the shear strain. Then, Hooke's law is written as $f/A = G\gamma$, where G is called shear modulus or rigidity.

Next, let us consider the volume change of a spherical elastic body (volume v) which is surrounded by liquid. When the liquid pressure is raised from p to $p+\Delta p$ by a pump, the volume of the sphere will decrease from v to v-δv. Then, Hooke's law is written as $\delta p = -\kappa\ \delta v/v$. Since it is the custom to represent the sign of the compressional pressure as positive, the negative sign in the right-hand side originates from the decrease of the volume under compression. Here, κ is called bulk modulus, and its inverse $1/\kappa$ is called compressibility.

When a cylinder of length l and the radius r is extended to its axial direction without any force at side surface, the radius will be decreased from r to r-δr. The ratio of the transverse strain $-\delta r/r$ to the longitudinal strain $\delta l/l$ is called Poisson's ratio μ: $\mu = -(\delta r/r)/(\delta l/l)$. The negative sign originates from the fact that when the length of cylinder is increased ($\delta l > 0$), the radius is decreased ($\delta r < 0$). Generally, the value of Poisson ratio ranges from 0.5 for incompressible material like rubber to 0 for porous material like cork.

The Relation Among Four Elastic Parameters E, G, κ, and μ

Commonly used four elastic constants E, G, κ, and μ are not independent, and are related with each other as shown in Table 3.1. Only two constants are independent, and therefore, when two constants are determined the other two can be calculated. On the other hand, the determination of only one constant is not complete to understand the whole elastic property of that material.

As mentioned above, the Poisson ratio μ ranges from 0 to 0.5. In Table 3.1, the bulk modulus κ is given as a function of E and μ. When μ approaches 0.5, the denominator $(1 - 2\mu)$ approaches to zero and thus the bulk modulus approaches to infinity, therefore, the bulk modulus is much larger than the other elastic parameter G and E. This is just the case for rubber. The fact that the bulk modulus is much larger than G and E means that this material needs a very high pressure to reduce the volume, hence this is called an incompressible material. In such a case, Young's modulus is about three times of the shear modulus: $E = 3G$.

Shear deformation appears in the torsion, and can be determined by the measurement of the moment. The deformation mode is the same as in rotational viscometer.

When a beam is bent by an applied couple, an upper part is stretched and the lower part is compressed. There is a part near the middle layer which retains the

original length, and is called a neutral layer. Then, Young's modulus is involved in the bending, and is obtained from the determination of the sag.

Since measurement of bending is easy, it is often used to study rheological properties of solids. To apply three point bending test to a soft matter such as agarose gels, the points were replaced by cylindrical rods (Bonn et al. 1998).

Strain energy of elastic materials is given by the elastic modulus $\times$ (strain)^2/2 for all deformation modes, elongation, shear, and expansion.

Poisson's ratio of most engineering solids, metals, plastics, and glasses is known to be about 0.3 while those of many soft foods such as cheese and jellies are reported as 0.5 just like a rubber. Cork and flexible foams show no lateral expansion when compressed thus their Poisson's ratio is very close to zero. Poisson's ratios of vegetables and fruits are reported higher than those of metals and plastics but lower than those for cheese and jellies, for example, 0.37 for an apple tissue (Powel 1994). It is also important to take into account the deformation rate (in most cases compression is selected), since the real food is not purely elastic but rather viscoelastic, and shows a time dependence. When a 1.33% gel of gellan was compressed slowly at 0.005 mm/min, no lateral expansion was observed (Nakamura et al. 2001).

3 Viscosity: Newtonian Fluid

There are many models for viscous fluids, and a Newtonian fluid is the simplest model. In this model, the tangential stress is written by a linear equation of the shear rate.

Imagine the fluid is filled between the lower and the upper plates (Fig. 3.2). When the upper plate is moved to the right direction parallel to the x-axis, the fluid in the neighborhood of the upper plate is dragged with the plate, and the fluid far from the upper plate is dragged with a slower velocity.

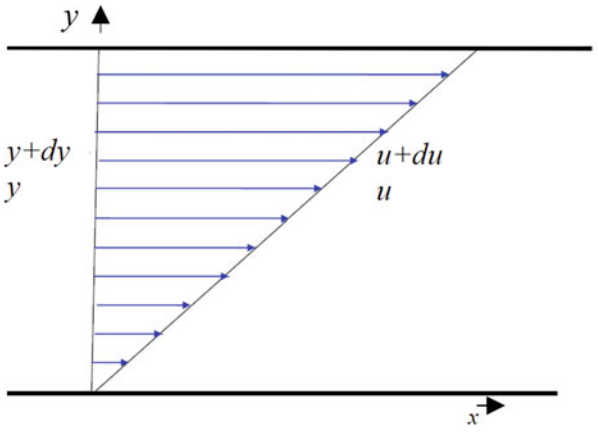

Fig. 3.2 Fluid flow in a narrow gap δ between two very large planes. Upper plate (y = δ) moves parallel to x-axis. Lower plate (x-axis) is fixed at y = 0. Velocity gradient $\partial u/\partial y$ is given by shear rate dγ/dt because the shear γ is dx/dy, and the velocity u is dx/dt

The velocity vector is written as $u = [u(y), 0, 0]$. In the Newtonian fluid, the tangential stress τ is proportional to the velocity gradient, $\partial u/\partial y$, the change in the velocity of the fluid flow in the direction perpendicular to the direction of fluid flow, $\tau = \eta \partial u/\partial y$, where the proportional coefficient η is called viscosity. This is called a Newton's law of viscosity. When a constant shear stress is given, the velocity gradient $\partial u/\partial y$ is small for a fluid of which the viscosity is large. The viscosity represents the tangential stress which is required to produce the unit velocity gradient, thus it is the resistance to the flow.

The viscosity of the fluid can be determined by various methods as described below.

3.1 Capillary Viscometer

Let us imagine a fluid flow in a capillary. Symmetrical considerations indicate that the velocity distribution in the liquid will be symmetrical around the axis of the capillary, and have its maximum value on this axis. Flow rate Q of a Newtonian fluid (viscosity η) in a capillary (radius a and length l) under a pressure difference Δp is given by

$$Q = \int_0^a 2\pi r u \, \mathrm{d}r = \pi \Delta p a^4 / 8\eta l$$

taking into account that u is the flow velocity at r (the distance from the axis $r = 0$), and $2\pi r\mathrm{d}r$ is the area of the circular ring from r to $r+\mathrm{d}r$. The flow velocity $u = (\Delta p/4\eta l)\ (a^2 - r^2)$ takes maximum at the central line $r = 0$, and becomes slower with increasing distance from the central line. The viscosity of the liquid can be determined by measuring Q, volume V of liquid flowing through the capillary in time t, i.e. $Q = V/t$. This is called Hagen–Poiseuille equation.

3.2 Falling Ball Viscometer

This is the simplest evaluation of the sedimentation of food particles in the suspension and creaming in the emulsion. Imagine a solid sphere (radius a and density ρ) is falling slowly at a velocity v in a surrounding infinite medium (viscosity η, density ρ_0). The frictional force exerting on the falling sphere is given by Stokes law $6\pi a\eta v$ when the velocity is slow. When the falling velocity is constant (acceleration is zero), the upward force and downward force should be balanced, and thus the falling velocity v is given by

$$v = \frac{2a^2}{9\eta}(\rho - \rho_0)g$$

where g is the gravitational acceleration. When the density of the sphere ρ is lower than that of the medium ρ_0, the sphere will float up, and the floating velocity can be calculated in the same way. If the spherical material is not a solid but immiscible liquid such as in the case of creaming up oil droplet in water, the coefficient in the Stokes formula is given by $4\pi a\eta$ instead of $6\pi a\eta$. If the sphere is a gas bubble, this coefficient is known to be closer to the solid sphere $6\pi a\eta$ rather than to that of the liquid sphere because the surface of the bubble is usually covered with a hard layer.

Various rotational viscometers are used: liquid samples are put between the cone and plate in cone plate viscometers, and samples are put between an inner cylinder and an outer cylinder in coaxial cylindrical viscometers (called also Couette viscometers).

3.3 Reynolds Number

In the above-mentioned viscometers, viscosity can be determined only for a laminar flow in which the fluid moves in parallel layers. In the laminar flow, the streamlines show regular shapes and do not intersect each other. In fluid flow of high velocity, the flow becomes turbulent where the fluid shows a non-regular motion and the velocity at any point varies in both direction and magnitude with time. Turbulent motion is accompanied by the formation of eddies and the rapid interchange of momentum in the fluid. The change from the laminar flow to turbulent flow occurs at a critical value of Reynolds number Re: $\mathrm{Re} = \rho vl/\eta$, where ρ is the density of the fluid, η is the viscosity of the fluid, v is the velocity of the fluid in motion relative to some solid body characterized by a linear dimension l (called characteristic dimension).

$$\mathrm{Re} = \frac{\rho vl}{\eta} = \frac{\rho l^3 (v^2/l)}{\eta (v/l) l^2} = \frac{\text{mass} \times \text{acceleration}}{\text{viscosity} \times \text{shear rate} \times \text{area}} = \frac{\text{inertial force}}{\text{viscous force}}$$

Thus, the physical meaning of Reynolds number is the ratio of the inertial force to the viscous force. Characteristic length represents the radius or the diameter for spheres, and is an equivalent diameter (or radius) for non-spherical objects. The equivalent radius is defined for non-spherical objects based on Stokes' law. The Reynolds number is used to predict the transition from laminar flow to turbulent flow.

4 Non-Newtonian Flow: Shear Thinning and Shear Thickening

Most liquid foods, except water, alcohol, oil, are not Newtonian fluids. Simple models frequently used to analyze the flow behavior of liquid foods are shown in Fig. 3.3.

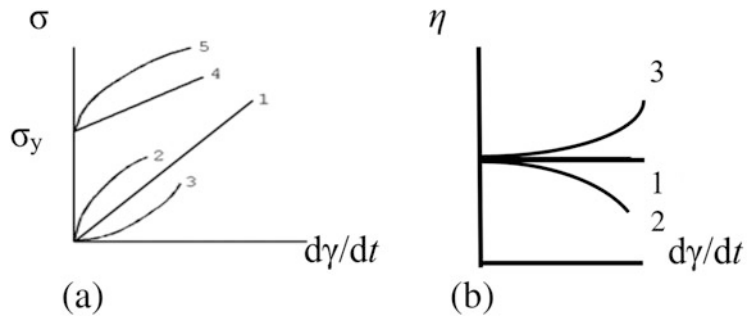

Fig. 3.3 (**a**) Shear stress plotted against shear rate for commonly used simple models of fluids. (1) Newtonian fluid $\sigma = \eta\ (d\gamma/dt)$, (2) Power law fluid (shear thinning) $\sigma = \eta\ (d\gamma/dt)^n$, $n < 1$, (3) Power law fluid (shear thickening) $\sigma = \eta\ (d\gamma/dt)^n$, $n > 1$, (4) Bingham fluid $\sigma = \eta\ (d\gamma/dt) + \sigma_y$, (5) Herschel–Bulkley fluid $\sigma = \eta\ (d\gamma/dt)^n + \sigma_y$. (**b**) Viscosity as a function of shear rate for Newtonian (1), shear thinning (2) and shear thickening (3) fluids

Newtonian fluid shows a linear relation between shear stress and shear strain, and the straight line for shear stress vs shear strain passes through the origin. The viscosity defined by the shear stress divided by shear strain for a power law fluid $\sigma = \eta\ (d\gamma/dt)^n$ with $n < 1$ decreases with increasing shear rate, and the behavior is called shear thinning (Model 2 in Fig. 3.3b). Most common liquids show such a behavior. Shear thinning may be attributed to many reasons depending on the sample structure: alignment of rod-like particles or molecules in the flow direction, disintegration of aggregated particles. The viscosity for a power law fluid with $n > 1$ increases with increasing shear rate, and the behavior is called shear thickening (Model 3 in Fig. 3.3b). There are not so many examples, but starch paste and some other examples are shown later.

Liquid foods filled in tubes such as mayonnaise or tomato ketchup or tooth paste do not begin to flow if it is not subjected to a certain stress. The minimum stress required to cause a flow is defined as yield stress. A fluid which has a yield stress and shows a linear stress–strain rate as in Newtonian flow above the yield stress is called a Bingham liquid (Model 4 in Fig. 3.3a). Hershel–Bulkley liquid is a fluid which has a yield stress and shows a non-linear stress–strain rate above the yield stress (Model 5 in Fig. 3.3a). Spreadability of butter, cream, jam, paste (legume, fish, meat, nuts, seed, spice, herb, etc.) is closely related with yield stress, and is discussed later.

In addition to these five models, the following Casson equation is also frequently used.

$$\sigma^{1/2} = {\sigma_c}^{1/2} + {\eta_c}^{1/2}(d\gamma/dt)^{1/2}$$

where σ_c and η_c are called the Casson yield stress and the Casson viscosity coefficient, respectively. The intercept of fitting line is square root of Casson yield stress. Casson yield stress is the minimum stress that is needed for the fluid to flow. Casson's equation has been widely used in the evaluation of chocolate.

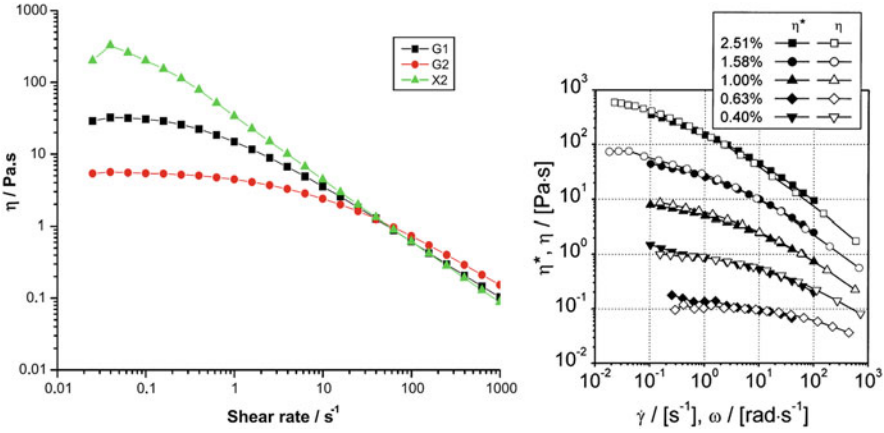

Fig. 3.4 (**a**) Shear rate dependence of the viscosity of xanthan and guar solutions showing the crossover at 50 s^{-1}. The shear rate was changed stepwise from 0.03 to 1000 s^{-1} for 10 min. Closed square G1, 2.0 wt% guar ($M_w = 1.4 \times 10^6$) solution; closed circle G2, 2.6 wt% guar ($M_w = 6.3 \times 10^5$). closed triangle, X2, 4.1 wt% xanthan ($M_w = 3.4 \times 10^6$) solution. Reproduction with permission from Nishinari et al. (2011), Copyright 2011 Elsevier. (**b**) Cox–Merz plot for aqueous solution of hydroxypropylmethyl cellulose ($M_w = 2.6 \times 10^6$) with different concentrations. Complex viscosity η^* is defined in Sect. 5. Reproduction with permission from Clasen and Kulicke (2001). Copyright 2001 Elsevier

4.1 Steady Shear Viscosity of Polymer Solutions

Polysaccharide thickening agents show shear thinning behavior. Xanthan is a microbial polysaccharide consisting of a linear (1–4) linked β-D-glucose backbone with a trisaccharide chain on every other glucose at C-3, containing a glucuronic acid residue linked (1–4) to a terminal mannose unit and (1–2) to a second mannose that connects the backbone, and has also been used widely in food industry as a thickener and texture modifier because its solution is stable over a wide pH and temperature range (Sworn 2021). The persistence length of xanthan was determined as 120 nm (Sato et al. 1984) and it explains well why this polysaccharide is an excellent thickener. Guar is one of galactomannans consisting of a mannan backbone and galactose side chains (Nishinari et al. 2007). The ratio of mannose to galactose is approximately 2:1. Rheological and related characteristics of guar have been extensively studied, and Mark–Houwink–Sakurada exponent and the persistence length are reported as 0.7 and 4 nm, respectively (Picout and Ross-Murphy 2007; Picout et al. 2001). In comparison with corresponding data 0.65 and 2.5 nm for a standard flexible polysaccharide, pullulan (Nishinari et al. 1991; Shingel 2004) it is evident that guar is slightly stiffer and its solution with the same molar mass and concentration shows higher viscosity than that of pullulan.

Steady shear viscosity of aqueous solutions of guar gum and xanthan gum solutions as a function of shear rate is shown in Fig. 3.4a. Xanthan solution shows pronounced shear thinning as reported by many previous workers. An apparent shear thickening behavior at lower shear rate is caused by structural formation after the

preparation of solution and it does not appear in the curve observed by lowering the shear rate. Wagner et al. (2016) recently reexamined this problem.

The lower molar mass guar shows less shear thinning and an apparent Newtonian plateau at lower shear rate as expected (Clasen and Kulicke 2001). This is consistent with previous data for guar gum fractions degraded enzymatically by β-mannanase for different times (Cheng and Prud'homme 2000).

When the complex viscosity $\eta^* = G^*/i\omega$ (Sect. 5) as a function of angular frequency ω, and the steady shear viscosity η as a function of shear rate $d\gamma/dt$ are plotted, the so-called Cox–Merz plot, both viscosities coincide as shown in Fig. 3.4b. When the complex viscosity and the steady shear viscosity do not coincide, it may mean that the microstructure at the relaxed state is destroyed by shear force. Then, the steady shear viscosity at higher shear rate may be smaller than the corresponding complex viscosity. However, it should be reminded that more fine local structure cannot be detected by this method. It is yet useful to see the validity of Cox–Merz rule for solutions of thickening agents.

Richardson and Ross-Murphy (1987a, b) reported that 3% guar gum solutions obeyed the Cox–Merz rule, but xanthan solutions deviated from it, and they ascribed it to some microstructure, "weak gel" (although senior author of this paper regretted to use this term 20 years later and prefers to use "structured liquid" because it is not a gel) formation in xanthan solutions. While guar gum solutions can be "thickeners," xanthan solutions are "stabilizers" in which fine particles can be suspended without sedimentation. This suggests that some "structure" exists in xanthan solutions. Wientjes et al. (2000) did not find the validity of Cox–Merz rule for guar gum solutions. It is difficult to know the cause of the discrepancy between papers of these two groups.

Steady shear viscosity of xanthan solution has been studied extensively. Since xanthan chain is very stiff (persistence length 120 nm as mentioned above), the solution shows a shear thinning behavior. Yet, Einaga et al. (1977) show a Newtonian plateau at very low shear rates for a solution of much stiffer schizophyllan (persistence length 180 nm, $M = 4.3 \times 10^6$) in water at 30 °C using a Zimm–Crothers type viscometer.

It was shown that globular protein solutions do not obey the Cox–Merz rule (Ikeda and Nishinari 2001a, b).

One important reason why xanthan is widely used as a thickener and stabilizer is that its remarkable shear thinning behavior in comparison to galactomannans such as guar and locust bean gum (LBG) in addition to its insensitivity to the change in temperature and pH. The high viscosity at low shear rates makes xanthan a good stabilizer which suspends fine particles of herbs at rest, and the low viscosity at higher shear rate confers it a flowability in motion. Recently, the steady shear viscosity of bacterial cellulose (BC) was compared with that of xanthan and LBG, and it was found the BC solution was more shear thinning than xanthan solution even at a lower concentration (Paximada et al. 2016). BC is also reported to be a good suspending agent for chocolate drink preventing the precipitation of cocoa particles, and in addition BC has a great heating stability after sterilization and thus the viscosity remains unchanged after heat treatment (Shi et al. 2014). This potential of BC was not exploited so much although it has attracted more attention as a unique jelly dessert known as *nata de coco* or stabilizer of ice cream (Azeredo et al. 2019).

The occurrence of shear thickening depends on the phase volume, particle size (distribution), particle shape, as well as those of the suspending phase (Barnes 1989, 2000). The increase of the viscosity above a critical shear rate is ascribed to the transition from a two- to a three-dimensional spatial arrangement of the particles. After this transition, the viscosity decreases again with increasing further shear rate.

Shear thickening behavior in food systems has been overviewed (Bagley and Dintzis 1999). Suchkov et al. (1997) reported a shear thickening behavior of 11S broad bean globulin (legumin) in 0.6 mol/dm^3 NaCl at pH 4.8 which was shown to have an upper critical temperature of 21 °C and a critical protein concentration of 18%. Dintzis et al. (1996) reported that waxy starches (corn (maize), rice, barley, and potato) showed shear thickening to a greater extent than did wheat, normal rice or normal corn starches when dissolved gently and dispersed at 3.0% concentration in 0.2N NaOH.

Shear thickening was observed for a 17.22% schizophyllan (M_w = 450 kDa) solution around a shear rate of 0.01–0.1 s^{-1} (Fang et al. 2004b). At the same shear rate range, a steep change in the birefringence was observed indicating an abrupt increase in molecular orientation. This is due to the extreme stiffness of schizophyllan chain as mentioned above.

Recently, the classical most well-known corn starch suspension was revisited, and shown that the so-called walking on water effect could be observed only above 52.5 wt% (42 vol%); a 2.1 kg rock laid on starch suspension with different concentrations fell, but a falling rock was bounced when it hit the surface of the starch slurry of 52.5 wt% (Crawford et al. 2013).

Solutions of mamaku polysaccharide extracted from black tree fern were shown to show the shear thickening behavior (Goh et al. 2007). Another example of shear thickening behavior was reported for sulfated polysaccharides from seaweeds (Shao et al. 2014).

4.2 Concentration Dependence of Viscosity

To understand the concentration dependence of the viscosity of polymer solutions, it is necessary to take into account the molar mass, molecular conformation, and shear rate dependence as is described in Chap. 2. The concentration dependence of viscosity of flexible polymers is usually represented by the relation between zero shear specific viscosity and the coil-overlap parameter defined by the product ($C[\eta]$) of the concentration (C) with the intrinsic viscosity [η]. Morris et al. 1981 Here, the intrinsic viscosity is determined by the extrapolation of the specific viscosity to zero concentration. The specific viscosity η_{sp} is defined as $\eta_r - 1$, where the relative viscosity η_r is defined as the ratio of the viscosity of the solution to that of the solvent η_s: $\eta_r = \eta/\eta_s$.

As shown above, most polymer solutions are non-Newtonian fluids and show a shear thinning behavior. At sufficiently low shear rate, the viscosity does not depend on the shear rate and shows a Newtonian plateau, so the viscosity observed at the

shear rate extrapolated to zero can be obtained, and it is called simply a zero shear viscosity (η_0).

As described above, some models have been proposed to interpret the shear rate dependence of the viscosity of polymer solutions most of which are non-Newtonian liquids. Cross model is widely used to fit the observed shear rate dependence where both the zero shear viscosity η_0 and the infinite shear viscosity η_∞ are observed:

$$\frac{\eta - \eta_\infty}{\eta_0 - \eta_\infty} = \frac{1}{1 + (K\dot{\gamma})^m},$$

where K has the dimension of time, and m is dimensionless. The value of m ranges from 0 to 1, and represents the degree of shear thinning. When m is closer to zero it tends to more Newtonian liquids, while the most shear thinning liquids have a value of m tending to unity.

Some other models Carreau model, Sisko model, etc. are also used (see more different models in Barnes (2000) and Lapasin and Pricl (1999)). Risica et al. (2010) used Cross eq to analyze the shear rate dependence of guar gum and hydroxypropylmethyl guar aqueous solutions.

The double logarithmic plot of the zero shear specific viscosity (η_{sp0}) of polymer solutions and polymer concentration shows two straight lines. The slope of these straight lines is smaller at lower concentrations than at higher concentrations, and the crossover point C^* of these straight lines shifts to lower concentrations with increasing molar mass of a polymer.

Irrespective of chain flexibility, the slope at lower concentrations is reported as ca.1 and the slope at higher concentrations as 3.3 for many polysaccharides, but some other slopes are also reported and tabulated in Lapasin and Pricl 1999. When the zero shear specific viscosity is represented by a power law ($\eta_{sp,0} \sim C^n$), the exponent (n) takes different values below and above C^*. The exponent n for most polysaccharide solutions ranges from 1.1 to 1.6 below C^*, and from 1.9 to 5.6 above C^* (tabulated in Lapasin and Pricl 1999).

4.3 Salt Effect

The viscosity of polyelectrolyte solutions is influenced strongly by the presence of salt. In contrast to the common procedure to determine the intrinsic viscosity of non-electrolytic polymers, the reduced viscosity (η_{sp}/C) of polyelectrolyte solutions shows a turn up in the extrapolation of polymer concentration. It is caused by the polymer coil expansion by electrostatic repulsion. By adding salt, the reduced viscosity decreases and the extrapolation to zero concentration becomes possible. See, for example, the zero shear rate reduced viscosity vs. equivalent monomer concentration of sodium pectate at various counterion concentrations (Lapasin and Pricl (1999)). Smidsrød and Haug (1971) proposed an empirical method to determine the stiffness parameter B by determining the intrinsic viscosity at 0.1M ionic strength (See Chap. 2). While the viscosity of flexible polyelectrolye solutions is

decreased by the addition of salt, that of stiff chains such as xanthan is comparatively insensitive to the addition of salt because the volume occupied by the stiff chain in the solution is not so much reduced as in the case of flexible chains. This comparative insensitivity/stability of the viscosity is one of the reasons why xanthan is used widely in food processing as mentioned before.

Wyatt et al. (2011) reported that the zero shear viscosity of xanthan showed different behaviors in the presence of salt depending on the polymer concentration. They observed that the zero shear viscosity of dilute xanthan solutions (500 ppm and 50 ppm) decreased while that of concentrated solution (4000 ppm) increased significantly by the addition of salt (50 mM NaCl). They also observed a similar behavior for anionic polysaccharides carrageenan and welan and also for a cationic polysaccharide chitosan. They stated that these results could be understood by scaling theories. Wyatt et al. (2011) found that Cox–Merz rule was valid for xanthan solutions, which is contradictory with previous reports by Lee and Brant (2002) and Richardson and Ross-Murphy (1987b), and they attributed this disagreement to the difference in the concentration.

4.4 Viscosity of Suspensions

The viscosity of dilute suspensions is well described by Einstein's equation $\eta = \eta_0 (1 + 2.5\varphi)$, where η_0 is the viscosity of a suspending medium, and φ represents the volume fraction of the dispersed phase. Figure 3.5 shows the normalized viscosity

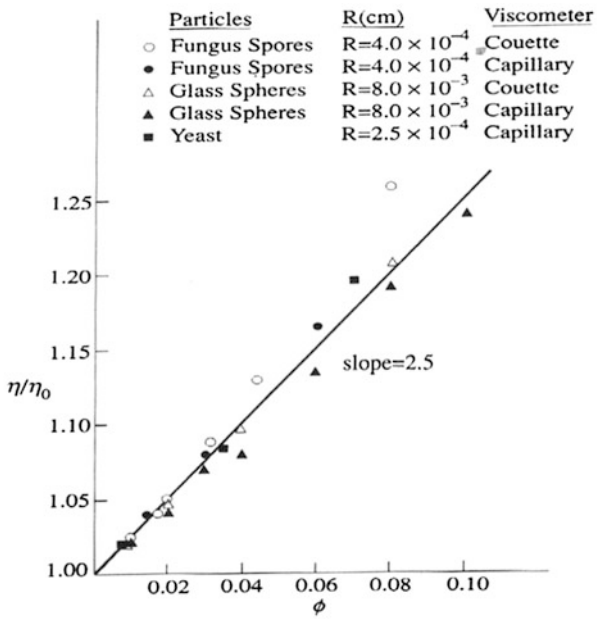

Fig. 3.5 Verification of Einstein's equation. Reproduction with permission from Hunter (1998). Copyright 1998 Oxford University Press

(the ratio of the viscosity of the suspension to that of the solvent) vs. the volume fraction for various materials. It is striking that this equation holds well irrespective of the different nature of materials tested, spores, glass, and yeast. It is dependent only on the volume fraction.

This equation does not hold, however, for concentrated suspensions, and various modified equations have been proposed (Hunter 1998).

4.5 Extensional Viscosity

There have been many studies on the extensional viscosity but less than those on shear viscosity because of the difficulty in the measurements. Methods of measurements are stretching liquid between two flat plates, cylindrical viscoelastic filament uniaxially extended by rotating clamp, crossed slot devices, and opposed jets (Barnes 2000, p. 160; Larson 1999, p. 19). While the shear viscosity is defined by $\eta_s = \tau/\dot{\gamma}$ where τ is the shear stress and $\dot{\gamma}$ is the shear strain rate, the extensional viscosity is defined by $\eta_e = \sigma/\dot{\varepsilon}$ where $\dot{\varepsilon}$ is the extensional strain rate. In Newtonian fluids, it is known that $\eta_e = 3\eta_s$. However, most food fluids are non-Newtonian, and the ratio of η_e/η_s, which is called Trouton ratio, is generally greater than 3. When a stick or a plate in a viscous liquid such as sugar syrup or honey is pulled up, the liquid flows downward and does not flow upward because they are Newtonian fluids. But, imagine the suspending of egg white just after cracking an eggshell or drooling from the mouth of a baby. Both of these liquids egg white/ saliva flow downward but then flow upward because of their elasticity. Egg white plays a role of cushion for an egg yolk and saliva and other mucins in humans have their own biological function which cannot be achieved if they are Newtonian liquids.

Chan et al. (2007) performed a comparative study of shear and extensional viscosity of casein, waxy maize, and their mixtures. They measured the extensional viscosity by observing the filament thinning when the liquid filament was extended. Chan et al. (2007) found that the maximum stretchable length of casein, waxy maize, and their mixtures were well described by a master curve using a capillary number (the product of the viscosity and the stretching speed divided by the surface tension) for viscous fluids, but the more concentrated samples showed a deviation from this master curve indicating the important effect of viscoelasticity.

Extensional viscosity of thickening agents has attracted much attention recently in relation with developing dysphagic treatments. Thickening agents are widely used in hospitals to prevent the aspiration. Thickening of a thin liquid such as tea, juice, or soup is effective (Cichero 2013). In addition to the increase of the viscosity, the cohesiveness of the liquid is believed to be necessary for safe swallowing, and the liquid extension test is suitable for this (Nishinari et al. 2019).

5 Viscoelasticity

Simple mechanical models consisting of a spring which obeys the *Hooke's elasticity* law $\sigma = G\,\varepsilon$ (σ stress; G elastic modulus; ε strain) and a dashpot which obeys the *Newtonian viscosity* law $\sigma = \eta d\varepsilon/dt$ (η viscosity) are used widely. A spring represents an ideal elastic body which deforms instantaneously (without delay) and recovers to the initial state when the external force is removed. A dashpot is an ideal viscous material where the shear stress σ is proportional to the shear rate $d\varepsilon/dt$. In the shear deformation, τ and γ are used for stress and strain in most textbooks.

Viscoelasticity is a relaxational phenomenon which depends on the time scale of the measurement. Typical viscoelastic phenomena are stress relaxation and creep. In the former, when the constant strain is given to a viscoelastic material, the induced stress decreases with the lapse of time, and it is called stress relaxation. In the latter, when a viscoelastic material is subjected to a constant stress, the induced strain increases with the lapse of time, and it is called creep. In these experiments, the stimulus causing the response is step-like and kept constant (does not depend on the time), and then, this is called static viscoelasticity.

A simple model consisting of a spring and a dashpot combined in series is called a *Maxwell element*. When a stress σ is applied to this model, the total strain ε is the sum of strains of each element, spring, and dashpot, and the total stress is equal to the stress of each element $\sigma = \sigma_1 = \sigma_2$ because they are combined in series. Therefore, $\sigma = G\varepsilon_1 = \eta d\varepsilon_2/dt$, where the suffixes 1 and 2 refer to the spring and dashpot, respectively. Substituting these into $\varepsilon = \varepsilon_1 + \varepsilon_2$, the relation between stress and strain (called *constitutive equation*) for a Maxwell element is obtained: $d\varepsilon/dt = (1/G)(d\sigma/dt) + (\sigma/\eta)$. A Maxwell model represents a liquid-like viscoelasticity because it shows an infinite deformation because of the dashpot. When this viscoelastic material is subjected to a step strain at time $t = 0$, the stress is decreased with the lapse of time. This phenomenon is called *stress relaxation*. The above Maxwell eq gives the solution for this phenomenon, $\sigma(t) = \varepsilon_0 G e^{-t/\tau}$, where $\tau = \eta/G$ is called the *relaxation time*, indicating that the stress decreases exponentially.

A simple model consisting of a spring and a dashpot combined in parallel is called a *Kelvin–Voigt element*. When a stress σ is applied to this model, the total stress σ is the sum of stresses of each element, and the total strain is equal to the strain of each element, $\varepsilon = \varepsilon_1 = \varepsilon_2$ because they are combined in parallel. Therefore, $\sigma_1 = G\varepsilon_1$ and $\sigma_2 = \eta d\varepsilon_2/dt$, respectively. Substituting these into $\sigma = \sigma_1 + \sigma_2$, the constitutive equation for a Kelvin–Voigt element is obtained: $\sigma = G\varepsilon + \eta d\varepsilon/dt$. A Kelvin–Voigt model represents a solid-like viscoelasticity in spite of the presence of a dashpot because it is combined in parallel with the spring which shows only a finite deformation. When a viscoelastic material is subjected to a step stress σ_0 at time $t = 0$, the strain is increased with the lapse of time. This phenomenon is called *creep*. The above Kelvin–Voigt eq gives the solution, $\gamma(t) = (\sigma_0/G)\,[1\text{-}\exp(-t/\tau_r)]$, where $\tau_r = \eta/G$ is called *retardation time*. The retardation time is the time at which the strain reaches (1-1/e) times the final strain (σ_0/G) after an infinite time.

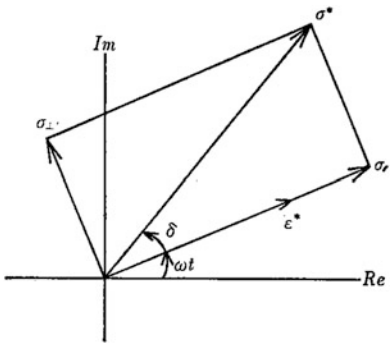

Fig. 3.6 Strain vector ε^* and stress vector σ^* on the complex plane. ε^* rotates around the origin with constant angular velocity ω, while σ^* also rotates with the same ω with a leading phase δ. $\sigma_{//}$ and $\sigma_{\perp}$ show stress components with the same phase and the leading phase to ε^*

In real material, the two element model such as Maxwell element and Kelvin–Voigt element cannot describe well the rheological behavior. Assume that the strain $\varepsilon(t)$ of the material subjected to the constant stress σ_0 at time $t = 0$ is proportional to σ_0, then $\varepsilon(t) = \sigma_0 J(t)$ where $J(t)$ is called *creep compliance*. When $J(t)$ does not depend on σ_0, this material behavior is called linear. If σ_0 is doubled, $\varepsilon(t)$ induced by the stress is also doubled in this case.

$J(t)$ consists of three parts:

$$J(t) = J_0 + J_d\,\varphi(t) + t/\eta\ (*)$$

where J_0 is the instantaneous compliance which obeys Hooke's law, t/η is the viscous flow following the Newton's law, and the $J_d\,\varphi(t)$ is the retarded elasticity, and $\varphi(t)$ is called creep function, $\varphi(0) = 0$, $\varphi(\infty) = 1$. This is generally valid irrespective of the model. The creep function is given by $\varphi(t) = 1 - \exp(-t/\tau_r)$. These parameters can be determined graphically.

Dynamic Viscoelasticity

In the dynamic viscoelastic measurements, the viscoelastic material is subjected to the sinusoidal strain or stress, and the induced sinusoidal stress or strain is observed. The oscillational stress and strain can be represented in complex plane as vectors rotating at an angular velocity ω as shown in Fig. 3.6, where δ is the phase difference.

The shear strain is written as $\gamma^* = \gamma_0 \exp(i\omega t) = \gamma_0\, e^{i\omega t}$, and the shear stress is $\sigma^* = \sigma_0\, e^{i(\omega\, t\, +\, \delta)}$. The complex elastic modulus is defined by $G^* = \sigma^*/\gamma^*$. Therefore, $G^* = (\sigma_0/\gamma_0)e^{i\delta} = (\sigma_0/\gamma_0)\,(\cos\delta + i\,\sin\delta)$.

When G^* is written as $G' + iG''$, the real part G' is called storage modulus, and the imaginary part G'' is called loss modulus.

$$G' = (\sigma_0/\gamma_0)\ \cos\ \delta, G'' = (\sigma_0/\gamma_0)\ \sin\ \delta$$

The ratio G''/G' is called mechanical loss tangent $\tan\delta = G''/G'$, which is related to the energy loss as shown below.

Complex viscosity is defined by

$$\eta^* = G^*/\mathrm{i}\omega = \eta' - \mathrm{i}\,\eta''$$

And its absolute value is $|\eta^*| = [(G')^2 + (G'')^2]^{1/2}/\omega$
$\eta' = G''/\omega$, $\eta'' = G'/\omega$

For some polysaccharide solutions, the so-called Cox–Merz rule, which states that the complex viscosity plotted vs angular frequency agrees with the steady shear viscosity plotted vs shear rate, holds as is shown in Fig. 3.4b. But, this rule is an empirical rule with no sound theoretical validation, and many deviations are also reported.

Dynamic Behavior of Maxwell Element and Kelvin–Voigt Element
When a sinusoidal strain $\varepsilon_0 e^{\mathrm{i}\omega t}$ is given to a Maxwell element, the frequency dependence of complex modulus is given by

$$G_{\mathrm{M}}^*(\mathrm{i}\omega) = \frac{\mathrm{i}\omega\tau G}{1 + \mathrm{i}\omega\tau}$$

and the storage and loss moduli are

$$G_M'(\omega) = G\frac{\omega^2\tau^2}{1 + \omega^2\tau^2}$$
$$G_M''(\omega) = G\frac{\omega\tau}{1 + \omega^2\tau^2}$$

When a sinusoidal stress $\sigma_0 \mathrm{e}^{\mathrm{i}\omega t}$ is given to a Kelvin–Voigt element, the frequency dependence of complex compliance is given by

$$J_{\mathrm{KV}}^*(\mathrm{i}\omega) = \frac{1}{G}\frac{1}{1 + \mathrm{i}\omega\tau}$$

Loss Modulus is Related to the Energy Loss
Question: Calculate the energy dissipated in a viscoelastic material during one period of oscillation, and show that it is proportional to G''

Answer

$$\int_0^{\frac{2\pi}{\omega}} \eta\dot{\gamma}\frac{d\gamma}{dt}dt = \int_0^{\frac{2\pi}{\omega}} \eta\dot{\gamma}^2 dt = \int_0^{\frac{2\pi}{\omega}} \eta(\gamma_0\omega\cos\omega t)^2 dt = \eta\omega^2{\gamma_0}^2\frac{\pi}{\omega} = \pi{\gamma_0}^2\omega\eta = const G''$$

Mechanical Spectra: Frequency Dependence of Storage and Loss Moduli
Frequency dependence of storage and loss moduli for polymer solutions or colloid dispersions can be classified into four categories as shown in Fig. 3.7. In the dilute solutions where polymers dissolve with little or no overlap with each other, $G' < G''$

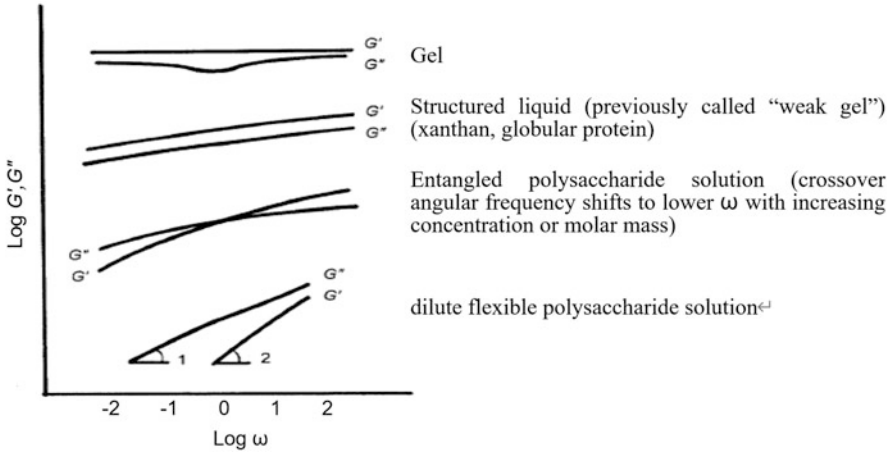

Fig. 3.7 Typical angular frequency ω dependence of G' and G'' of commonly used thickening agents. It should be noted that values of G' and G'' depend not only on the concentration but also on the molar mass and conformation of hydrocolloids or the coil-overlap parameter

and at very low frequencies it is seen that $G' \sim \omega^2$, $G'' \sim \omega$. At higher concentrated solutions $G' < G''$ at lower frequencies, but at higher frequencies $G' > G''$ and thus at an intermediate frequency the crossover $G' = G''$ is observed. This is interpreted as follows: at higher frequencies entangled polymer chains play a knot of temporary network and thus somewhat a solid-like behavior is observed, but at lower frequencies, the time of oscillational period is long enough for chains to disentangle, and thus it shows a liquid-like behavior $G' < G''$. The transition from the dilute region to entangled region is seen by the coil-overlap parameter = intrinsic viscosity × polymer concentration as mentioned before. For networks or elastic gels, $G' > G''$ at a wider frequency range and tan $\delta < 0.1$. Between an elastic gel and concentrated (entangled) polymer solutions, another frequency dependence is observed, and it is called a structured liquid. This frequency dependence is also seen in globular protein solutions. Previously, it was called a weak gel. But, as will be discussed in detail in the next chapter, it is essentially a liquid and flows above a yield stress, which is discussed later in this chapter.

Time–Temperature Superposition

As is well known a material behaves like a liquid for a slow deformation, and shows a solid-like behavior for a fast deformation (see e.g. https://en.wikipedia.org/wiki/Pitch_drop_experiment). We also know that many solids become soft or firm when heated or cooled. For many synthetic polymers, the data obtained at low (high) temperatures are equivalent to those obtained at a high (low) frequency or a short (long) time scale, and then it was found that the data can be superposed by shifting horizontally (parallel to the time or temperature axis). When such a superposition between time and temperature is possible, it is called *thermorheologically simple*, and the resulted curve is called a *master curve*. The time–temperature superposition was successfully applied to many synthetic polymers, but great caution is needed to apply to food biopolymers.

Lissajous–Bowditch Figure and LAOS (Large Amplitude Oscillatory Shear) When the sinusoidal stress and strain, $\sigma = \sigma_0 \sin\omega t$ and $\gamma = \gamma_0 \sin\omega t$, are taken as x-axis and y-axis in the orthogonal coordinate system, the Lissajous–Bowditch figure is obtained. In the elastic material, the stress and strain are in phase, and the Lissajous–Bowditch figure is a straight line. In the viscous material, the stress and strain are $\pi/2$ out phase, and the Lissajous–Bowditch figure is a circle. In the viscoelastic material, the stress and strain are δ out of phase, and the Lissajous–Bowditch figure is an ellipse.

Generally, the linear viscoelastic range is wider for flexible linear polymer solutions than for structured liquids. Beyond the linear viscoelastic range, the resulted Lissajous–Bowditch figure is skewed. While the deviation from the elliptical shape is very small for a concentrated polysaccharide solution (hydroxyethyl guar gum), a pronounced distortion was recognized for a structured liquid (sc1eroglucan) particularly at low frequency (Lapasin and Pricl 1999).

To understand quantitatively the non-linear viscoelastic behavior of food materials, large amplitude oscillatory shear (LAOS) has recently been attracting much attention. LAOS behaviors are often shown by the strain dependence of G' and G'' at a constant angular frequency ω, and are classified into four types: (1) strain thinning (G' and G'' decreasing); (2) strain hardening (G' and G'' increasing); (3) weak strain overshoot (G' decreasing, G'' increasing followed by decreasing); (4) strong strain overshoot (G' and G'' increasing followed by decreasing) (Hyun et al. 2011). However, this presentation cannot capture and clarify the whole characteristics of non-linear rheology. Chebyshev polynomial presentation has been proposed to get more physical meaning from LAOS data (Cho et al. 2005; Ewoldt et al. 2008).

The elastic (σ') and viscous (σ'') stress are given by

$$\sigma'(x) = \gamma_0 \sum_{n:\ \text{odd}} e_n(\omega, \gamma_0)\, T_n(x)$$

$$\sigma''(x) = \gamma_0 \sum_{n:\ \text{odd}} v_n(\omega, \gamma_0)\, T_n(y)$$

where $T_n(x)$ is the nth order Chebyshev polynomial of the first kind, $T_1(x) = x$, $T_3(x) = 4x^3 - 3x$, $T_5(x) = 16x^5 - 20x^3 + 5x$, $\cdots$

and $x = \gamma/\gamma_0$, $y = \dot{\gamma}/\dot{\gamma}_0$, provide the appropriate domains of $[-1, +1]$ for orthogonality, $e_n(\omega, \gamma_0)$ and $v_n(\omega, \gamma_0)$ are elastic and viscous Chebyshev coefficients.

In the Fourier representation of LAOS, the stress response $\sigma(t; \omega, \gamma_0)$ to the strain stimulus $\gamma(t) = \dot{\gamma}_0 \sin\omega t$ or strain rate stimulus $\dot{\gamma}(t) = \dot{\gamma}_0 \sin\omega t$ is given by

$$\sigma(t;\omega,\gamma_0) = \gamma_0 \sum_{n\ \text{odd}} \left\{ G'_n(\omega,\gamma_0) \sin n\omega t + G''_n(\omega,\gamma_0) \cos n\omega t \right\},$$

$$\sigma(t;\omega,\gamma_0) = \dot{\gamma}_0 \sum_{n\ \text{odd}} \left\{ \eta''_n(\omega,\gamma_0) \sin n\omega t + \eta'_n(\omega,\gamma_0) \cos n\omega t \right\}.$$

The relationships between the Chebyshev coefficients in the strain or strain rate domain and the Fourier coefficients in the time domain are given by

$$e_n = G'_n\,(-1)^{(n-1)/2} \quad n : \text{odd},$$
$$v_n = G''_n/\omega = \eta'_n \quad n : \text{odd},$$

In the linear regime at small strains, $e_3/e_1 << 1$ and $v_3/v_1 << 1$, and the linear viscoelastic relations

$$e_1 \to G' \text{ and } v_1 \to \eta' = G''/\omega.$$

are obtained. The strain-stiffening ratio S and the shear thinning ratio T are defined as follows:

$$S = \left(G'_{\mathrm{L}} - G'_{\mathrm{M}}\right)/G'_{\mathrm{L}} = (4e_3 + \ldots.)/(e_1 + \mathrm{e}_3 + \quad)$$
$$T = \left(\eta'_{\mathrm{L}} - \eta'_{\mathrm{M}}\right)/\eta'_{\mathrm{L}} = (4v_3 + \ldots.)/(v_1 + \mathrm{v}_3 + \quad)$$

where G'_{L} and G'_{M} are large strain modulus and minimum strain modulus respectively;

$$G'_M \equiv \left.\frac{d\sigma}{d\gamma}\right|_{\gamma=0} = \sum_{n\ \text{odd}} nG'_n = e_1 - 3e_3 + \cdots,$$
$$G'_L \equiv \left.\frac{\sigma}{\gamma}\right|_{\gamma=\pm\gamma_0} = \sum_{n\ \text{odd}} G'_n(-1)^{(n-1)/2} = e_1 + e_3 + \cdots,$$

For a linear elastic response, $S = 0$ and $S > 0$ means intracycle strain stiffening. For a linear elastic response, $T = 0$ and $T > 0$ means intracycle shear thickening.

LAOS studies on dough and gluten gels have been done using this method (Ng et al. 2011; Yazar et al. 2017a).

The characteristic shapes of Lissajous–Bowditch figures for a gluten gel over a range of strain amplitudes from $\gamma_0 = 0.02$ to 6.0 at a fixed angular frequency at $\omega = 1.0$ rad s^{-1} are plotted in Fig. 3.8 (Ng et al. 2011).

At smaller strain amplitudes, the relation between the stress and strain appears as an ellipse:

$$\sigma^2 - 2\sigma\gamma G' + \gamma^2\left(G'^2 + G''^2\right) = G''^2\gamma_0^2,$$

This quadratic form can be diagonalized, and the major and minor axes of the ellipse are centered at the origin. The enclosed area is given by $\pi{\gamma_0}^2 G''$, indicating the energy lost during one cycle of oscillation. As the strain amplitude is increased, the material response and shape of the Lissajous–Bowditch curves shown in Fig. 3.8 deviate significantly from this simple behavior. First a gradual "softening" of the

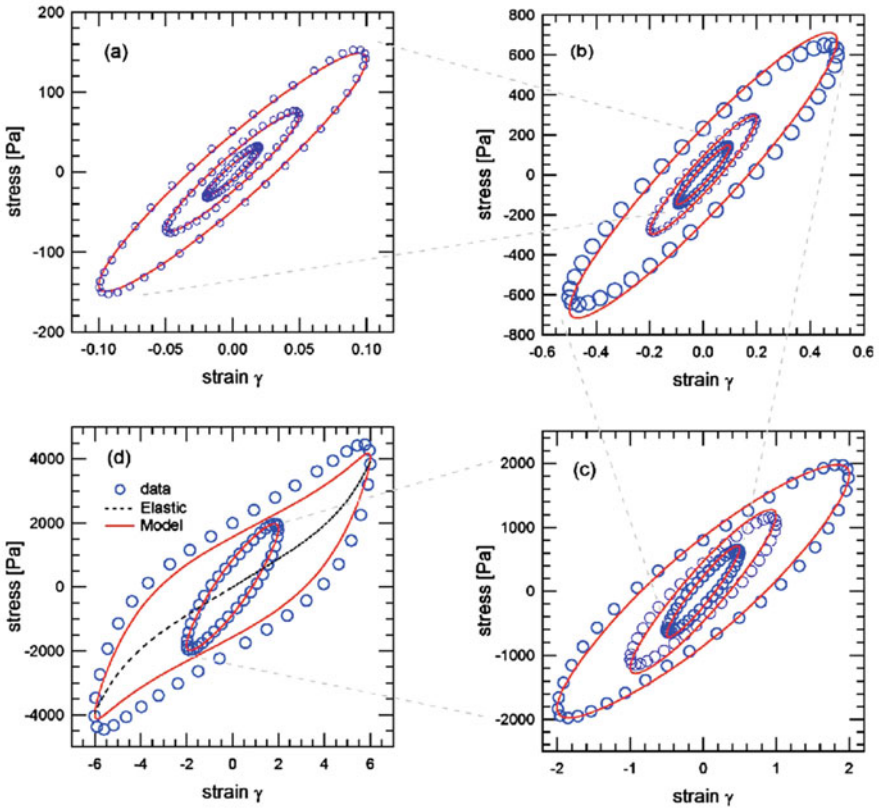

Fig. 3.8 Lissajous–Bowditch curves after 12 oscillatory cycles for a gluten gel at a fixed angular frequency $\omega = 1.0$ rad s^{-1} with (**a**) $\gamma_0 = 0.02, 0.05, 0.10$; (**b**) $\gamma_0 = 0.10, 0.20, 0.50$; the curve for $\gamma_0 = 0.10$ from (**a**) is repeated. (**c**) $\gamma_0 = 0.50, 1.00, 2.00$; (**d**) $\gamma_0 = 2.0$ and 6.00. As the imposed strain amplitude γ_0 increases from (**a**) to (**d**), the magnitude of the maximum stress grows and the axes are rescaled. Experimental data are plotted as open symbols. The decomposed elastic stresses are shown in the lower panel as a dotted line for $\gamma_0 = 6$. Predictions from the nonlinear generalized gel model are plotted as a solid line for each strain amplitude. Reproduction with permission from Ng et al. (2011). Copyright 2011 AIP

material is indicated by the clockwise rotation of the major axis toward the strain-axis. Second, a distinct "stiffening," indicated by the upturn of the shear stress, is observed at large strains (Fig. 3.8d). The magnitude of the enclosed area also increases with increasing amplitude, indicating an increasingly dissipative response. These non-linear features cannot be fully captured by simply reporting G' and G'' as a function of strain amplitude, as is usually done in linear viscoelasticity analysis (Ng et al. 2011).

Duvarci et al. (2017) applied this method to suspensions, emulsions, and elastic networks (tomato juice, mayonnaise, soft and hard dough). In the strain dependence of G' and G'' at a constant angular frequency, tomato paste showed the type (I), strain thinning (G' and G'' decreasing) while mayonnaise showed the type (III), weak

strain overshoot (G' decreasing, G'' increasing followed by decreasing). A slight strain softening ($S < 0$, $e_3/e_1 < 0$) at smaller strains and strain hardening at larger strains were observed for tomato paste and mayonnaise. Strain hardening ($e_3/e_1 > 0$) and shear thinning ($v_3/v_1 < 0$) were observed for soft dough and hard dough.

Biaxial deformation has been widely used in baking investigation, and gluten doughs showing high resistance to biaxial deformation and pronounced strain hardening behavior were found to be good for baking, i.e., larger bread volume (Kokelaar et al. 1996). Bread volume has been used as an index of the bread forming performance of dough. Recently, bread volume of gluten-free flour doughs were plotted as a function of large strain modulus G'_{L} or minimum strain modulus G'_{M}, and it was found that the bread volume increased with increasing G'_{L} and or G'_{M} (Yazar et al. 2017b).

6 Yield Stress

The concept of yield stress is intuitively evident: most fluid foods filled in tubes such as mayonnaise, mustard, ketchup, pastes, etc. begin to flow only when they are subjected to a certain value of stress. The minimum stress required to cause flow is the yield stress. The first simplest model is a Bingham fluid: $\sigma = \eta_{\mathrm{B}}\,(d\gamma/dt) + \sigma_y$, where σ_y is the yield stress, η_{B} is the Bingham plastic viscosity. Another simple model, Herschel–Bulkley fluid $\sigma = \eta_{\mathrm{HB}}\,(d\gamma/dt)^{\mathrm{n}} + \sigma_y$ has also been used for better describing the behavior.

Yield stress governs the thickness of coated chocolate on the biscuit as shown below (Fig. 3.9).

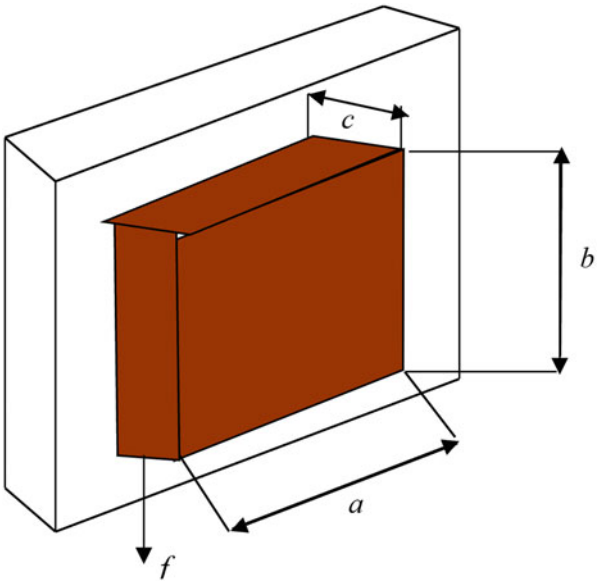

Fig. 3.9 Chocolate coating on biscuit. The yield stress of chocolate dictates the thickness of chocolate

The gravitational force exerting on the melted chocolate f is given by $f = mg = V\rho g$, where m is the mass, $V = a \times b \times c$ is the volume, ρ is the density of the chocolate. From the definition of the yield stress, this gravitational force should balance with the yield stress × surface area $= \tau_y \times a \times b$

Therefore, $a \times b \times c \times \rho \times g = \tau_y \times a \times b$

The thickness c of the chocolate is $c = \tau_y/\rho g$

For a chocolate with $\tau_y = 5$ Pa, $\rho = 1.06 \times 10^3$ kg/m^3, the thickness of the chocolate is given by

$$c = 5\ \mathrm{N\ m^{-2}}/\left(1.06 \times 10^3\ \mathrm{kg/m^3} \times 9.8\ \mathrm{m\ s^{-2}}\right) = 0.00048\ \mathrm{m} = 0.48\ \mathrm{mm}.$$

Yield stress can in principle be determined by decreasing the shear rate in the plot of the shear stress vs shear rate. Then, the shear stress obtained at zero shear rate is the yield stress. Rigorously speaking, it is impossible to determine the absolute yield stress which is conceptually the *idealization*. In a very long time scale everything flows even at a very low stress (Barnes 1999).

Although it is not easy to measure, the concept of the yield stress is meaningful in food science and technology, and it should be reminded that the yield stress values obtained by different methods can be compared only over the same range of shear rates (Barnes 1999; Bonn et al. 2017).

Many papers have been published on the existence of the true yield stress. Using four model yield stress materials, 0.2% carbopol, a commercial hair gel (containing carbopol, water triethanolamine as a stabilizing agent), a commercial shaving foam, and a cosmetic water-in-oil emulsion (composed of 80% water with carbopol 940 (1%) in Vaseline oil (6%) and Polyethylene glycol 600 (6%) with several additives, so that it remains stable under shear when used), Mϕller et al. (2009) showed that the yield stress really exists and it marks a transition between the fluid which flows and the solid which does not flow. These four samples are called "simple" yield stress materials because the viscosity depends only on the shear rate, and the yield stress is a material property while for thixotropic yield stress materials the viscosity depends also on the shear history, which is discussed in the next Sect. 7. "Apparent" viscosity = stress/(instantaneous shear rate) which is time dependent and therefore not "true" viscosity, of all the four materials as a function of stress showed a steep rise with decreasing stress and then leveled off to show a plateau value below a certain stress. The plateau value of the apparent viscosity increased with the measurement time up to ~10^3 s. Fig. 3.10a shows the apparent viscosity of 0.2% carbopol as a function of time for different stress values.

Above the stress 27 Pa, the apparent viscosity quickly reaches the steady value and then it stays constant up to ~10^3 s, while below the stress 25 Pa, the apparent viscosity continues to increase even at 10^4 s. Therefore, above the stress 27 Pa, the material flows at a constant viscosity which is a decreasing function of the stress, while the apparent viscosity continues to increase with time as $\eta \sim t^{0.6}$ as indicated by the dashed straight line, indicating that the system behaves almost as a solid having a very large viscosity within the experimentally accessible observation time. Thus, this stress 27 Pa can be defined as a yield stress. The same phenomenon was also observed for other three different materials. Below a critical stress, the viscosity

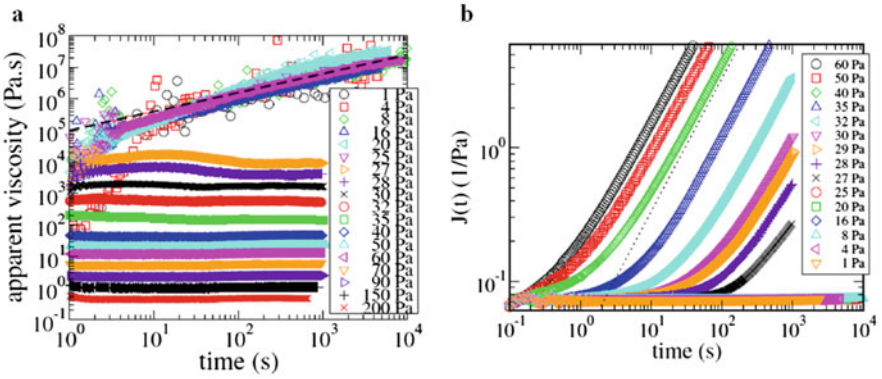

Fig. 3.10 (**a**) Apparent viscosity of 0.2% carbopol as a function of time at different stresses. At and above the stress 27 Pa, the apparent viscosity η of the sample shows a constant value (time independent) while at and below the stress 25 Pa, η increases with increasing time $\eta \sim t^{0.6}$ as indicated by the dashed straight line. (**b**) A creep compliance $J(t)$ of the same data as in left figure. At large t a fluid state will have a slope of 1 (indicated by the dotted line), while a solid state will have a slope of 0. At stresses of 27 Pa and above, slopes are nearly 1, while they are nearly 0 at 25 Pa and below—data for six stresses are collapsed and hardly discernable. Reproduction with permission from Mϕller et al. (2009). Copyright 2009 IOP

increases in time; the material eventually stops flowing. Above the critical stress, the viscosity decreases continuously in time; the flow accelerates. Thus the viscosity jumps discontinuously to infinity at the critical stress. This phenomenon is thus called viscosity bifurcation (Coussot et al. 2002a, b)

As shown clearly in Fig. 3.10b, at and below the stress 25 Pa the deformation was zero indicating the solid behavior below this critical stress (yield stress), while the compliance increases with increasing time with the slope 1 indicating the fluid behavior at and above the stress 27 Pa. Both Fig. 3.10a, b show clearly the existence of the yield stress, and this is also recognized also in the other three different yield stress materials, a hair gel, a shaving foam, and a water-in-oil emulsion.

Many methods have been proposed to determine the yield stress. Dinkgreve et al. (2016) using the same four model simple yield stress materials compared the yield stress values, and concluded that the Herschel–Bulkley fit to the stress-shear rate gives the lowest and the most reliable value for the yield stress. Vane geometry is sometimes useful to determine the yield stress because it is free from slippage (Stokes and Telford 2004).

7 Thixotropy

The viscosity of many structured liquids at a constant shear rate decreases with the lapse of time, which is called thixotropy. It is different from shear thinning behavior which is defined as the decreasing of the viscosity when the shear rate is increased.

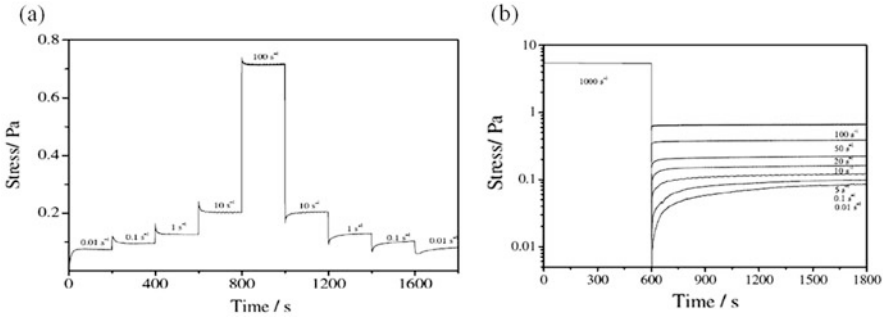

Fig. 3.11 (**a**) Shear stress transients in step shear rate tests for 6 wt% gum arabic in water. The shear rates of different steps were shown in the panel (**b**) Time evolution of the transient shear stress in sudden reduction of shear rate from 1000 s^{-1} to different lower shear rates for 6 wt% gum arabic solution. The different lower shear rates were shown in the panel. Reproduction with permission from Li et al. (2011). Copyright 2011 Elsevier

All the shear thinning liquid show a thixotropic behavior since it takes a time to recover the initial microstructure even if it is short.

Thixotropy is a time dependent rheological phenomenon, and it is understood as the microstructural formation at rest and the breakdown of that structure during shearing. The thixotropy is explained by the competing two processes *aging* (structure formation) and *rejuvenation* (structure breakdown).

Delayed failure of fish myosin gels was studied, and the time to failure as a function of scaled applied stress showed two regimes (Brenner et al. 2013). This time depends on the bond reformation rate; the time is short when the stress is high and bond reformation is not sufficient while it is long when the stress is low and bond is reformed (Sprakel et al. 2011; Lindstrom et al. 2012).

A hysteresis loop test which records a stress–shear rate curve is a simple demonstration of the thixotropic behavior and has been used widely for many foodstuffs such as yogurt. Although a loop test, shear stress vs shear rate, has been frequently used to study thixotropic behavior because it is easy to do, Barnes (1997) depreciated this method. Though it gives some qualitative information, he recommends the stepwise experiments where the shear rate or stress is changed from one constant value to another with a carefully controlled prehistory. The advantages of the stepwise change of shear rate in comparison with the hysteresis loop method are that not only the initial condition can be well-defined and reproducible, but also the shear rate during the actual test remains constant. Hence, the effect on an established structure of shearing at a fixed shear rate can be measured as a function of time (Mewis and Wagner 2012).

Figure 3.11 shows an example of such an experiment for solutions of gum Arabic which is widely used as emulsifiers and stabilizers in food industry. When the shear rate is increased/decreased in a step-like manner, the induced stress shows an overshoot/undershoot, and then decreases/increases to a stationary value. The transient stress shown in Fig. 3.11 can be written

$$\sigma = \frac{1}{\left[\frac{1}{\sqrt{\sigma_s}} + \left(\frac{1}{\sqrt{\sigma_i}} - \frac{1}{\sqrt{\sigma_s}}\right)\exp\left(-kt\right)\right]^2}$$

where σ_i and σ_s represent the initial and stationary values of the stress, respectively, and k is a kinetic constant with $k = k_f + k_b$. Here, k_f and k_b are rate constants, which modulate the kinetics of structural buildup and breakdown processes, respectively. The rate constant k_f depends on temperature, whereas k_b is a function of the applied shear rate, and t is the testing time. Although old textbooks describe a gum Arabic solution as a Newtonian solution, the recent improvement of the rheometry makes it possible the measurement at low shear rates. The deviation from the Newtonian behavior at low shear rates ($<10\ s^{-1}$) suggests the existence of the molecular aggregation which is broken down by shear flow. The above equation was also used by Grassi et al. (1996) for scleroglucan and by Fang et al. (2004a) for schizophyllan. Oleogel consisting of rapeseed oil and shellac (a resin secreted by an insect) also showed a thixotropic behavior (Patel et al. 2013). This indicates that an oleo gel is a structured liquid and not a gel as defined in the next chapter. Actually, this oleo gel shows a flow behavior without fracturing when it is subjected to shear which is widely observed for structured liquids with yield stress such as xanthan, welan, rhamsan, schizophyllan, and scleroglucan.

The stepwise experiment to examine the thixotropic nature of low-fat mayonnaise-like emulsion gels, containing egg yolk, rapeseed oil (30% instead of 80% in full-fat mayonnaise), salt, sugar, vinegar, and 4.0% alginate solution and KGM powder, was performed (Yang et al. 2020). Structural recoverability was found for the low-fat mayonnaise-like emulsion gels in the stepwise experiment, and the stackability was enhanced by adding small amount of calcium ions. Stackability is required for mayonnaise, and is related with yield stress.

The opposite behavior of thixotropy is called *antithixotropy* where start-up flow or a sudden increase in shear rate causes an *increase* in viscosity over time (Mewis and Wagner 2012).

The dilute solution of globular protein shows another unique aspect, an antithixotropic rheological behavior; the viscosity of beta-lactoglobulin solutions at a fixed low shear rate increased with the lapse of time (Renard et al. 1996).

8 Microrheology

In the conventional or bulk rheology, the sample size is generally mm order and 1 cm^3 in volume, and therefore it is difficult to get the information of local region of inhomogeneous sample. Microrheology is useful to examine the rheological properties of a local region in inhomogeneous materials such as cytoplasm, thick egg white, and emulsion gels. The idea to determine the elasticity and viscosity in inhomogeneous materials dates back to Freundlich and Seifriz, and Heilbronn in 1920s, and development of theories on Brownian motion and experimental

techniques, electronics, spectroscopy, light scattering, thereafter made the method more quantitative.

There are two types of measurements in microrheology: passive and active methods. The microrheological information obtained by these two methods are equivalent by virtue of the fluctuation–dissipation theorem (FDT) in the equilibrium state (Doi 2013; Waigh 2016; Yang et al. 2017).

In the passive microrheology, the mean square displacement (MSD) of the probe particle is detected and analyzed by video tracking, laser tracking, and diffusing wave spectroscopy.

Multi-particle tracking microrheology was performed to obtain local elasticity and heterogeneities of gellan microgels using fluorescent colloidal particles with diameter of 0.5 μm (Caggioni et al. 2007).

9 Fractional Calculus Bridging the Instrumental Measurement and Sensory Evaluation

9.1 Scott Blair's Approach to Understand the Firmness Judged by Humans

Intermediate materials between elastic solid and viscous fluid such as cheese cannot be characterized only by modulus or by viscosity. In most food rheology, the intermediate state of the elasticity and viscosity has been studied as viscoelasticity where the rheological behavior of such materials is analyzed by static or dynamic viscoelastic measurement such as creep, stress relaxation or oscillation measurement, and large deformation and fracture mechanics have also been studied. Scott Blair proposed alternative method to analyze the rheological behavior of foods and other industrial materials by virtue of the "principle of intermediacy" (Scott Blair 1969). Instead of the complex plane representation of the storage modulus and loss modulus, he proposes a Cartesian coordinate consisting of the modulus $G = \sigma/\varepsilon$ and the viscosity $\eta = \sigma/(\mathrm{d}\varepsilon/\mathrm{d}t)$ to explain the "principle of intermediacy." An intermediate material between the elastic solid and the viscous liquid can be represented in this plane as a vector $\varphi = d^k\varepsilon/dt^k$, where k is a fraction and $d^k\varepsilon/dt^k$ is a fractional derivative which Scott Blair introduced into rheology to understand the relation between the sensory assessment and the instrumental measurement. The elastic material with $k = 0$ is judged by the strain ε and the viscous material with $k = 1$ is judged by the strain rate, that is $d^1\varepsilon/dt^1$, and therefore, it is reasonable to think that the fractional differentiation of the strain $d^k\varepsilon/dt^k$ should be used for the judgment of the firmness for the materials with $0 < k < 1$ intermediate between the elastic material and the viscous material.

To represent the intermediate state of the elasticity and viscosity, the quasi-property χ was defined as (Scott Blair 1947)

$$\chi = \sigma/\left(d^k\varepsilon/dt^k\right)$$

where $d^n\varepsilon/dt^n = \psi^{-1}\ \sigma\ k(k\text{-}1)\ (k\text{-}2)\cdots(k\text{-}n{+}1)\ t^{(k\text{-}n)} = \psi^{-1}\ \sigma\ t^{(\text{k-n})}\ \Gamma(k{+}1)/\ \Gamma(k\text{-}n{+}1)$,
where, Γ(k-n+1) is a gamma function

$$\Gamma(\mathrm{k}+1) = \int_0^\infty e^{-z}z^k dz = \mathrm{k}\,\Gamma(\mathrm{k}) = \mathrm{k}(\mathrm{k}-1)\ (\mathrm{k}-2)\cdots(\mathrm{k}-\mathrm{n}+1)$$

Although most physicists had not agreed to use "quasi-properties," Reiner supported Scott Blair's concept.

The fractional calculus has been used to discuss the rheological properties of various soft materials (Koeller 1984; Jaishankar and McKinley 2012; Rogosin and Mainardi 2014). The mechanical element having an intermediate behavior of the spring and dashpot is called Scott Blair element or springpot model having a constitutive equation

$$\sigma = G\frac{d^\beta\gamma}{dt^\beta}\ (0 < \beta < 1)$$

Therefore, from the experimental observation of $J(t)$, or $G(t)$, or $G'(\omega)$ and $G''(\omega)$, parameters G and β of springpot model can be determined.

9.2 *Recent Development of the Application of Fractional Calculus to Liquid Foods*

Wagner et al. (2017) based on fractional calculus studied the rheological properties of thickening agents used in dysphagia. Fractional Maxwell model (FMM) and Fractional Jeffereys model (FJM) were used. FMM is a series combination of two springpots with quasi-properties V, α and G, β, and it is reduced to a spring or dashpot when $\alpha = 0$ or $\alpha = 1$, respectively. FJM is a parallel combination of FMM and a dashpot with the viscosity η_s.

The steady shear viscosity can be also written using these parameters. Wagner et al. (2017) used the Cox–Merz rule to correlate the small amplitude oscillational data of G' and G'' with the steady shear viscosity, and they found generally a good agreement although they needed some corrections taking into account the viscosity at higher shear rate. They fitted the experimental data of polysaccharide thickening solutions used for dysphagic treatment, a commercial thickener TUC and saliva, using the above equations, and obtained the parameters V, α, G, β and η_s of fractional models. They replaced G with K, and β with n, where K is the so-called consistency index of the fluid in the power law fluids (Curves 2 and 3 in Fig. 3.3a). Instead of η in power law models (2) and (3) in Fig. 3.3a, K is often used and called consistency index (with the unit of Pa s^n), while n is called flow behavior index (dimensionless).

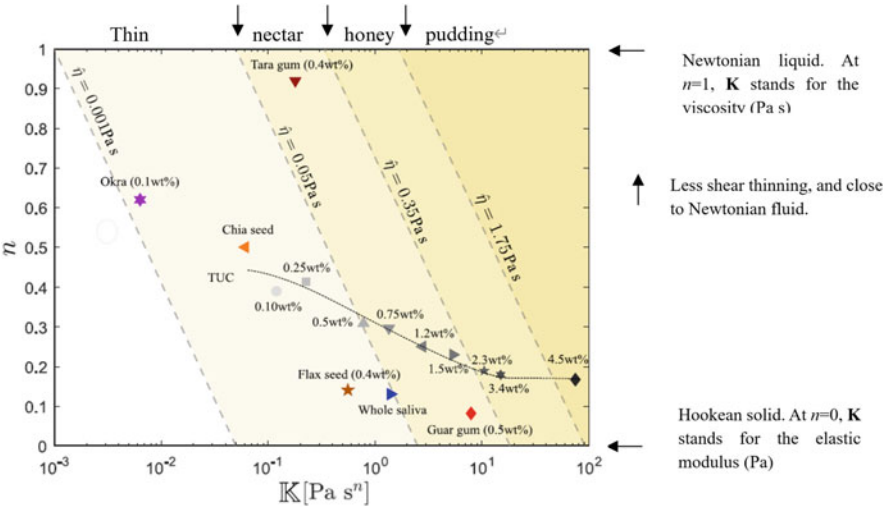

Fig. 3.12 Fractional parameter phase space for food consistency. The markers correspond to the values of the quasi-property $\boldsymbol{K}$ and fractional exponent n best describing the shear thinning in the steady shear viscosity of the TUC solutions, polysaccharides, and whole saliva at $\dot{\gamma} = 50\ s^{-1}$. The dashed diagonal lines bordering the shaded regions denote isoviscosity curves at $\dot{\gamma} = 50\ s^{-1}$ corresponding to the "thin" (0.001–0.05 Pa s) "nectar-like" (0.05–0.35 Pa s), "honey-like" (0.35–1.75 Pa s), and "pudding-like" (>1.75 Pa s), preparations of starch solutions by the National Dysphagia Diet Task Force. Reproduction with permission from Wagner et al. (2017). Copyright 2017 Elsevier

They analyzed the thickening behavior of various polysaccharides and a commercially available thickening agent TUC using fractional calculus power law model using the Cox–Merz rule

$$n(\dot{\gamma})|_{\dot{\gamma}=\omega} = |\eta^*(\omega)| = \mathrm{K}\omega^{\mathrm{n}\text{-}1}$$

In the fractional calculus treatment of viscoelasticity, K is called quasi-property. They found an excellent fitting using this equation for thickeners and plotted the data in the K-n plane (Fig. 3.12). K is taken as an abscissa and n is taken as an ordinate. The exponent $n = 1$ corresponds to the purely Newtonian viscous liquid, and $n = 0$ corresponds to a Hookean elastic solid. Each point in the interior of this parameter space in the range $0 < n < 1$ represents viscoelastic power law fluids.

In this K-n plane, equations of the dashed diagonal straight lines are

$$\mathrm{n} = 1 + \frac{\log \overline{\eta}}{\log 50} - \frac{\log K}{\log 50}$$

where $\overline{\eta} = 0.001$, 0.05, 0.35, and 1.75 from the left to right, and the slope of the diagonal straight lines is $-1/\log 50$.

As is seen clearly from Fig. 3.12, it is evident that the characterization of the "thickness" of these fluids only by the viscosity is insufficient. Tara gum is close to

the $n = 1$ Newtonian line, but the other fluids flax seed, whole saliva, guar gum, and TUC are all below $n = 0.5$, and elasto-plastic or yield stress like response is very important. The importance of the elastic contribution for the dysphagia treatment is in good agreement with the concept that cohesiveness of bolus is important for safe swallowing (Nishinari et al. 2019). The advantage of the analysis based on fractional analysis is that it contains only a few parameters which can be determined by the well-defined rheological measurements.

Faber et al. (2017a, b) studied the texture of cheese using the fractional calculus. They favored their approach based on the springpot model over the more undirected approach of statistically correlating large amounts of rheological data to the results from quantitative descriptive analysis (QDA) of multiple texture attributes. Their reservations to the latter approach are for two reasons. First the deformations and observations in QDA that lead to the texture judgment are ill-defined and may vary from subject to subject. This a priori weakens correlations with the measurements obtained from the carefully designed rheological experiment. Their second argument to favor the fractional calculus approach is that material properties are intrinsic properties whereas texture attributes are extrinsic in nature (Reiner 1971).

10 Further Developing of Thickening Properties

10.1 Viscosity of Mixed Hydrocolloids

The viscosity of the mixture of hydrocolloids has been studied from a long time ago. The so-called synergistic interaction between xanthan and guar, the viscosity of mixed solution as a function of mixing ratio showed a maximum, was reported (Sanderson 1981). The word synergism is used when the viscosity of the mixture is higher than the sum of the viscosities of the individual gum dispersions. However, in most cases, the viscosity of the mixture is lower than the sum, for example, the viscosity of mixtures of konjac glucomannan with xanthan, guar gum, carrageenan, sodium alginate, methyl cellulose, hydroxymethyl cellulose, sodium carboxymethyl cellulose, all the mixture except with xanthan showed the lower viscosity than the sum of the individual polysaccharide (Liang et al. 2011).

Recently, Zhang et al. (2015) examined the interaction of corn fiber gum (CFG) with various polysaccharides, hyaluronan (HA), guar gum (GG), carboxymethylcellulose (CMC), hydroxyethyl cellulose (HEC), konjac glucomannan (KGM), pectin, and chitosan using a shear stress synergy index I_s, which is defined by

$$I_s = \frac{\overline{\sigma}_{i+j}}{\overline{\sigma}_i + \overline{\sigma}_j},,$$

where $\overline{\sigma}_{i+j}$, $\overline{\sigma}_i$ and $\overline{\sigma}_j$ represent the shear stress for the mixture of i and j, i alone and j alone in the flow curve $\sigma \sim \dot{\gamma}$ written as follows:

$$\overline{\sigma} = \frac{1}{\dot{\gamma}_2 - \dot{\gamma}_1} \int_{\dot{\gamma}_1}^{\dot{\gamma}_2} \sigma d\dot{\gamma},$$

(Pellicer et al. 2000). This index I_s was used to judge whether the interaction is synergistic or antagonistic. When $I_s > 1$ it is judged as synergistic while when $I_s < 1$ it is judged as antagonistic or lack of synergism. Zhang et al. (2015) found the synergistic interaction, i.e. $I_s > 1$ for CFG with HA, HEC, GG, KGM, pectin, chitosan and concluded that CFG has a great potential as a viscosifying polysaccharide. CFG itself shows a very low viscosity and almost a Newtonian behavior like gum Arabic, while the interaction with other polysaccharides induces a greater viscosity.

As for the temperature dependence of viscosity of thickening agents, xanthan shows low temperature dependence and so stable, but in heat processing the viscosity lowering is sometimes required so that the stirring force can be weak. Xyloglucan (XG) is suitable for such requirement. Viscosity of tapioca starch (TS) suspension is reported to be more heat resistant when xyloglucan was added (Pongsawatmanit et al. 2006). The influence of temperature on the apparent viscosity of TS paste was estimated by an Arrhenius plot ln (viscosity) vs $1/T$. The activation energy E_a determined from the slope of this plot for TS mixed with XG was found much smaller than for TS alone, indicating that the addition of XG improved the heat stability. It was also found that the water separation from freeze-thaw samples was much reduced by XG.

Exactly the same reasoning was used in the same year 2006, to show the thermal stability of the mixture of hydroxypropyl-substituted guar (HPG) and carboxymethyl hydroxypropyl- substituted guar (CMHPG) in comparison with each individual HPG and CMHPG (Zhang and Zhou 2006). Zhang and Zhou found that the activation energy was smaller for the mixed CMHPG/HPG solution indicating that the mixture showed the improved temperature tolerance with respect to the viscosity. They also found that the viscosity of the 1:1 mixed solution was higher than that of each individual solution.

10.2 Molecular Structure and Viscosifying Function

The beneficial effect of dietary fibers is recognized well, and this function is generally believed to be conferred by high viscosity. However, in the supplement utilization, too high viscosity hinders the sufficient intake of dietary fibers, and therefore enzymatically degraded guar gums, degraded sodium alginate, dietary fiber from psyllium seed husk, and other polysaccharides have been commercialized (www.mhlw.go.jp/english/topics/foodsafety/fhc/02.html).

Cellulose chemists have modified the structure of cellulose by adding some residues at C2, C3, and C6 thus controlling the solubility and viscosifying properties.

Similar trials have been made for various polysaccharides using chemical and enzymatic modifications.

Recently, new variants of xanthan were created using genetic engineering (Wu et al. 2019). Since the shear rate dependence of these variants shows quite a different behavior, the further developments are expected.

Zhao et al. (2017) found that a new exopolysaccharide from a strain *Klebsiella* sp. is very resistant against the extreme pH. Although solutions of this new polysaccharide show a commonly observed shear thinning behavior at pH range from 2 to 12, this polysaccharide is degraded outside of this pH range. However, when the alkaline degraded polysaccharide is acidified into neutral pH, both moduli increased and the crossover was observed at pH 10.5. Below that pH, the solution showed a structured liquid behavior. It suggests that the backbone structure of this polysaccharide was not degraded, and some conformational change was reversible as observed in scleroglucan, which showed a rheological recovery induced by the partial recovery of triple helices from coil conformation after the degradation at high pH (Aasprong et al. 2003). The advantage of this new polysaccharide is that the viscosifying properties are stable and not so much changed by the addition of sodium, potassium, magnesium, and calcium ions as in xanthan.

11 Application of Hydrocolloids as a Thickener

11.1 Controlling the Viscosity and Stabilizing of Liquid Foods, Acidified Milk, Sauces

High methoxyl pectin (HMP) has been used widely to stabilize acidified milk drinks for over 60 years. Stabilization mechanism of HMP was attributed to the steric repulsion among HMP adsorbed casein aggregates and not by a weak gel network, and the adsorption of HMP to the surface of casein aggregates was by electrostatic attraction (Parker et al. 1994; Jensen et al. 2010). Kiani et al. (2010) studied the stabilization of a traditional Iranian yogurt drink by gellan/HMP, and suggested that gellan confers the additional stabilization effect. Recently, another pectic polysaccharide extracted from *Ulmus davidiana* was found effective to stabilize yogurt preventing syneresis and also promoting the growth of lactic acid bacteria (Yeung et al. 2019). Many other hydrocolloids with low viscosity such as soluble soybean polysaccharides (Maeda and Nakamura 2021), gum tragacanth, and Persian gum (Azarikia and Abbasi 2016) were also shown effective for the stabilization of acidified milk drinks. While low viscosity acidified yogurt drinks are liked by healthy young consumers, high viscosity ones are preferred by traditionalists and also believed to be safer for dysphagic patients in hospitals.

Since starch is the most widely used hydrocolloids, it is important to know the effect of seasonings on rheological properties. Hirashima et al. (2005, 2012) found

the great difference of the viscosities of 3 wt% maize starch suspensions/pastes to which sucrose, acids, and salt were added before and after the heating.

Xanthan is used frequently to thicken the starch paste. Caramel sauces made from potato starch containing glucose syrup were thickened by xanthan (Krystyjan et al. 2012). Xanthan was also added to tapioca starch paste to increase the viscosity and the stability against heating (Chantaro et al. 2013).

Low calorie mayonnaise using xanthan gum has been commercialized in Japan. A body mouthfeel should be maintained while reducing oil content in mayonnaise. The viscosifying function of xanthan surely plays an important role here, but its stability in acidic pH and the texture constancy in the presence of salt are also required. A good flavor release is also required and it is related with shear thinning behavior of xanthan. A mixture of xanthan, locust bean, guar and tamarind gums is used to make a tofu of higher water holding capacity and with a good mouthfeel. Xanthan is used to prevent retrogradation of rice-cake (*mochi*) and also to improve the texture. A thickener consisting of xanthan and low methoxyl pectin is proposed. Japanese noodles containing xanthan are reported to have an elastic texture. Xanthan is also used for glaze in order to protect frozen fish and vegetables preventing syneresis (Nishinari 1988).

Hanpen is a traditional fish product in Japan. It contains many air bubbles and has a sponge-like texture. Meat of sharks and cod are mashed with yams and then boiled in hot water. Sharks and yams are necessary for producing air bubbles. A traditional sponge cake containing many foams and with a moist mouthfeel, *Karukan*, also relies on yam polysaccharides. The foam producing and stabilizing capacity of yam polysaccharides is believed to originate from high viscosity but also from some elasticity.

Spinnability is related with the breakup length when the liquid is subjected to extension. When a glass rod is immersed into a liquid and then pulled up vertically, even sugar syrup which is very close to a Newtonian fluid shows a thread because a liquid adhering on the glass rod is flowing down, and when all the liquid flows down, the thread breaks. However, when the fluid has a certain elasticity, the fluid extends by rubber elasticity and when the fluid breaks, the suspending fluid jumps up because of the elastic recovery. Therefore, the maximum extendable length of the fluid depends on the ratio of the viscosity and elasticity, which is known as the relaxation time (See Sect. 5). This property of fluid is closely related with cohesiveness which plays an important role together with viscosity in the safe swallowing (Nishinari et al. 2019). Elongational measurement is important for evaluating the spinnability and thickened fluids used in dysphagic treatments (Turcanu et al. 2018) because it is related with not only viscosity but also with elasticity.

In some thickening application, the short texture is required rather than long texture. Here, the "short" means neat and tidy mouthfeel and the draining and dripping off in the processing, which can be quantified by the break up length when the liquid is subjected to extension. In the operation of spreading honey on the bread, long texture hampers it. Some patent proposes to mix agar to make the texture short. This short texture is also preferred in thick sauce for breaded cutlets, and xyloglucan is often used for such a requirement. This short texture is also

suitable in sauce for barbecued /grilled meat and for a round dumpling made from powdered rice.

Many polysaccharides such as arabinoxylans, cereal beta-glucans, chitin and chitosan, dextran, mesquite gum, pullulan as well as vegetable proteins and milk proteins are used as thickening as well as stabilizing and emulsifying agents in various foods (Nussinovitch and Hirashima 2019).

Although the detailed mechanism of aspiration in dysphagic patients is not yet understood, thickening of liquid foods has been found effective to reduce the risk of aspiration. Thickening slows the liquid flow so that the epiglottis may be able to close the airway to prevent the penetration of the food bolus, although this scenario was not demonstrated so well (Cichero 2013; Steele et al. 2015; Nishinari et al. 2016). Many kinds of thickening agents are commercially produced and used in hospitals and organizations for disadvantaged persons (IDDSI, International Dysphagia Diet Standardisation Initiative: https://iddsi.org/; Japan Care Food Conference: https://www.udf.jp/).

11.2 Rheological Control of Texture by Polysaccharide Thickeners: Noodles/Pasta and Breads

Noodles are popular foods especially in Asia, and pasta, spaghetti, and macaroni, etc. are also popular in Western countries. Rice noodles are popular in Vietnam, Thailand, and other Asian countries, and high amylose rice (long grain indica type) is suitable for noodles. Recently, to reduce the excessive inventory and promote the utilization of low amylose rice (short grain japonica type), hydrocolloids are added to powdered rice to improve the texture in Japan. Noodles from low amylose rice are evaluated too sticky and not enough firm. Nitta et al. (2018) compared the texture of rice noodles treated by Ca^{2+}-induced setting of alginate or LM pectin, and found that the stickiness was reduced and the firmness was increased by the addition of alginate or pectin. Kita et al. (2009) reported the similar improvement of the texture of japonica rice noodles by adding tamarind seed gum (TSG). They found that the decrease in hardness of noodles by frozen storage was reduced by the addition of TSG. Chitosan was also used for rice noodles (Klinmalai et al. 2017). Esterified tapioca starch was also used for salted noodles (Eguchi et al. 2014). Silva et al. (2013) examined the effect of adding various polysaccharides, guar gum, LBG, KGM, HPMC, and xanthan on the mechanical properties of sweet potato noodles containing broccoli powders. They found that shear modulus of noodles was lowest in noodles with hydroxypropyl methylcellulose (HPMC) and xanthan, which was attributed to the restriction of swelling of starch granules by these polysaccharides with high water binding capacity.

Dough rheology has been a very important applied rheology since the birth of rheology, and the relation between the bread making property and the rheological properties of dough has been extensively studied. Viscosifying hydrocolloids have

been widely used for this, but the relation between the viscosifying property and the final bread property is not so well understood. Gluten plays a crucial role in the baking to form and keep "cell" walls, and many hydrocolloids are expected to improve the baking performance, but it was only partially successful. Doughs showing a strain hardening behavior in extension test were affirmed to have a good bread making property (Kokelaar et al. 1996). Since glutenin was identified as a main gluten fraction which plays an important role in elastic and strain hardening properties of dough, instead of using gluten whey protein particles are mixed with wheat starch to make a dough showing a similar strain hardening behavior to a normal wheat dough (van Riemsdijk et al. 2011).

Application of hydrocolloids for rice bread has also been reported. It has attracted much attention to make the gluten-free bread since the celiac disease was recognized to be caused by gluten. Hydrocolloids at 1% and 2% w/w, pectin, carboxymethylcellulose (CMC), agarose, xanthan or oat β-glucan were added to rice flour for gluten-free bread (Lazaridou et al. 2007). The loaf volume is one of most important index for bread making quality and it was found that the incorporation of xanthan at 1% into the gluten-free breads did not change the loaf volume and at 2% supplementation level even decreased the volume; this formulation exhibited the lowest volume among all preparations. This was consistent with previous findings. Recently, however, in comparison of locust bean gum, guar gum, xanthan gum, tamarind seed gum, native gellan gum, dextrin, LM pectin, fermented cellulose CMC, konjac glucomannan, HM pectin, κ-carrageenan, ι-carrageenan, and λ-carrageenan in baking, the highest loaf volume was found when xanthan was used (Morimoto et al. 2015). HPMC, guar gum, pectin, xanthan gum, TSG were added to rice flour to make a gluten-free bread (Jang et al. 2018), and the authors concluded TSG gave the best bread among these hydrocolloids. The inconsistency among reported results may be due to the difference in the hydrocolloids because most commercially available polysaccharides have many variations: molar mass may be different, degree of substitutions or branching if any, cation type if it is charged polymers, etc. Therefore, unfortunately, it is impossible to compare directly the papers without confirming that the hydrocolloids used are the same or not in addition to the other factors such as mixing ratios and mixing conditions. This situation led Japanese workers to form a collaborative research group using the common samples of gellan to study the gelling and viscosifying properties as described in the next chapter for gelling properties.

Because of the issue of celiac disease, gluten-free pasta and bread have been investigated by many research groups which tried to use various hydrocolloids to improve the quality and especially textural properties (Padalino et al. 2016; Pahwa et al. 2016; Rai et al. 2018). Lynch et al. (2018) reviewed potential application of exopolysaccharides for gluten-free bread, and showed that the added dextran increased the specific volume and reduced the crumb hardness and extend the shelf life of the bread better than HPMC, which was attributed mainly to water binding ability of this high molar mass and branched dextran (Rühmkorf et al. 2012).

References

Aasprong E, Smidsrød O, Stokke BT (2003) Scleroglucan gelation by in situ neutralization of the alkaline solution. Biomacromolecules 4:914–921. https://doi.org/10.1021/bm025770c

Azarikia F, Abbasi S (2016) Mechanism of soluble complex formation of milk proteins with native gums (Tragacanth and Persian Gum). Food Hydrocolloids 59:35–44. https://doi.org/10.1016/j.foodhyd.2015.10.018

Azeredo HMC, Barud H, Farinas CS, Vasconcellos VM, Claro AM (2019) Bacterial Cellulose as a raw material for food and food packaging applications. Frontiers in Sustainable Food Systems. https://doi.org/10.3389/fsufs.2019.00007

Bagley EB, Dintzis FR (1999) Shear thickening and flow induced structures in foods and biopolymer systems. In: Siginer DA, De Kee D, Chhabra RP (eds) Advances in flow and rheology of non-Newtonian fluids. Elsevier, London, pp 63–86

Barnes HA (1989) Shear-thickening ("Dilatancy") in suspensions of nonaggregating solid particles dispersed in Newtonian liquids. Journal of Rheology 33:329–366. https://doi.org/10.1122/1.550017

Barnes HA (1997) Thixotropy - a review. Journal of Non-Newtonian Fluid Mechanics 70:1–33. https://doi.org/10.1016/S0377-0257(97)00004-9

Barnes HA (1999) The yield stress -a review or 'παντα ρει'- everything flows? Journal of Non-Newtonian Fluid Mechanics 81:133–178

Barnes HA (2000) A handbook of elementary rheology. University of Wales, Aberystwyth

Bonn D, Kellay H, Prochnow M, Ben-Djemiaa K, Meunier J (1998) Delayed fracture of an inhomogeneous soft solid. Science 280:265–267. https://doi.org/10.1126/science.280.5361.265.

Bonn D, Denn MM, Berthier L, Divoux T, Manneville S (2017) Yield stress materials in soft condensed matter. Reviews of Modern Physics 89:035005. https://doi.org/10.1103/RevModPhys.89.035005

Bourne MC (2002) Food texture and viscosity, 2nd edn. Academic Press, New York

Brenner T, Matsukawa S, Nishinari K, Johannsson R (2013) Failure in a soft gel: delayed failure and the dynamic yield stress. Journal of Non-Newtonian Fluid Mechanics 196:1–7. https://doi.org/10.1016/j.jnnfm.2012.12.011

British Rheologists Club (1942) Classification of rheological properties. Nature 149:702. https://doi.org/10.1038/149702a0

Caggioni M, Spicer PT, Blair DL, Lindberget SE, Weitz DA (2007) Rheology and microrheology of a microstructured fluid: the gellan gum case. Journal of Rheology 51:851–865. https://doi.org/10.1122/1.2751385

Cao Y, He J, Fang Y, Nishinari K, Phillips GO (2014) Interactions between Schizophyllan and Curdlan molecules in solutions. Bioactive Carbohydrates Dietary Fibre 3:89–95. https://doi.org/10.1015/j.bcdf.2014.03.002

Chan PSK, Chen J, Ettelaie R, Law Z, Alevisopoulos S, Day E, Smith S (2007) Study of the shear and extensional rheology of casein, waxy maize starch and their mixtures. Food Hydrocolloids 21:716–725. https://doi.org/10.1016/j.foodhyd.2007.02.001

Chantaro P, Pongsawatmanit R, Nishinari K (2013) Effect of heating-cooling on rheological properties of tapioca starch paste with and without Xanthan Gum. Food Hydrocolloids 13:183–194. https://doi.org/10.1016/j.foodhyd.2012.10.026

Chen J, Engelen L (eds) (2012) Food oral processing: fundamentals of eating and sensory perception. Wiley-Blackwell, Chichester

Cheng Y, Prud'homme RK (2000) Enzymatic degradation of guar and substituted guar galactomannans. Biomacromolecules 1:782–788. https://doi.org/10.1021/bm005616v

Cho KS, Hyun K, Ahn KH, Lee SJ (2005) A geometrical interpretation of large amplitude oscillatory shear response. Journal of Rheology 49:747–758. https://doi.org/10.1122/1.1895801

Cichero JAY (2013) Thickening agents used for dysphagia management: effect on bioavailability of water, medication and feelings of satiety. Nutrition Journal 12:54. https://doi.org/10.1186/1475-2891-12-54

Clasen C, Kulicke W-M (2001) Determination of viscoelastic and rheo-optical material functions of water-soluble cellulose derivatives. Progress in Polymer Science 26:1839–1919. https://doi.org/10.1016/S0079-6700(01)00024-7

Coussot P, Nguyen QD, Huynh HT, Bonn D (2002a) Viscosity bifurcation in thixotropic, yielding fluids. Journal of Rheology 46:573–589. https://doi.org/10.1122/1.1459447

Coussot P, Nguyen QD, Huynh HT, Bonn D (2002b) Avalanche behavior in yield stress fluids. Physical Review Letters 88:175501. https://doi.org/10.1103/PhysRevLett.88.175501

Cragg LH, Bigelow CC (1955) The viscosity slope constant k' of ternary systems: polymer–polymer–solvent. Journal of Polymer Science 16:177–191. https://doi.org/10.1002/pol.1955.120168208

Crawford NC, Popp LB, Johns KE, Caire LM, Peterson BN, Liberatore MW (2013) Shear thickening of corn starch suspensions: does concentration matter? Journal of Colloid and Interface Science 396:83–89. https://doi.org/10.1016/j.jcis.2013.01.024

Davies HS, Pudney PDA, Georgiades P, Waigh TA, Hodson NW, Ridley CE, Blanch EW, Thornton DJ (2014) Reorganisation of the salivary mucin network by dietary components: insights from green tea polyphenols. PLoS ONE 9:e108372. https://doi.org/10.1371/journal.pone.0108372

de Gennes PG (1979) Scaling concepts in polymer physics. Cornell University Press, Ithaca

Dealy J, Plazek D (2009) Time-temperature superposition - a users guide. Rheology Bulletin 78:16–31

Dinkgreve M, Paredes J, Denn MM, Bonn D (2016) On different ways of measuring "the" yield stress. Journal of Non-Newtonian Fluid Mechanics 238:233–241. https://doi.org/10.1016/j.jnnfm.2016.11.001

Dintzis FR, Berhow MA, Bagley EBWYV, Felker F (1996) Shear-thickening behavior and shear-induced structure in gently solubilized starches. Cereal Chemistry 73:638–643

Doi M (2013) Soft matter physics. Oxford University Press, Oxford

Duvarci OC, Yazar G, Kokini JL (2017) The comparison of LAOS behavior of structured food materials (suspensions, emulsions and elastic networks). Trends in Food Science and Technology 60:2–11. https://doi.org/10.1016/j.tifs.2016.08.014

Eguchi S, Kitamoto N, Nishinari K, Yoshimura M (2014) Effects of esterified tapioca starch on the physical and thermal properties of Japanese white salted noodles prepared partly by residual heat. Food Hydrocolloids 35:198–208. https://doi.org/10.1016/j.foodhyd.2013.05.012

Einaga Y, Miyaki Y, Fujita H (1977) A rotational viscometer permitting successive dilution. Nihon Reoroji Gakkaishi 5:188–193. https://doi.org/10.1678/rheology1973.5.4_188

Ewoldt RH, Hosoi AE, McKinley GH (2008) New measures for characterizing nonlinear viscoelasticity in large amplitude oscillatory shear. Journal of Rheology 52:1427–1458. https://doi.org/10.1122/1.2970095

Faber TJ, Jaishankar A, McKinley GH (2017a) Describing the firmness, springiness and rubberiness of food gels using fractional calculus. Part I: theoretical framework. Food Hydrocolloids 62:311–324. https://doi.org/10.1016/j.foodhyd.2016.05.041

Faber TJ, Jaishankar A, McKinley GH (2017b) Describing the firmness, springiness and rubberiness of food gels using fractional calculus. Part II: measurements on semi-hard cheese. Food Hydrocolloids 62:325–339. https://doi.org/10.1016/j.foodhyd.2016.06.038

Fang Y, Takahashi R, Nishinari K (2004a) Rheological characterization of schizophyllan aqueous solutions after denaturation– renaturation treatment. Biopolymers 74:302–315. https://doi.org/10.1002/bip.20081

Fang Y, Takemasa M, Katsuta K, Nishinari K (2004b) Rheology of schizophyllan solutions in isotropic and anisotropic phase regions. Journal of Rheology 48:1147–1166. https://doi.org/10.1122/1.1781170

Goh KKT, Matia-Merino L, Hall CE et al (2007) Complex rheological properties of a water-soluble extract from the fronds of the black tree fern, *Cyathea medullaris*. Biomacromolecules 8:3414–3421. https://doi.org/10.1021/bm7005328

Grassi M, Lapasin R, Pricl S (1996) A study of the rheological behavior weak gel systems. Carbohydrate Polymers 29:169–181

Hirashima M, Takahashi R, Nishinari K (2005) Changes in the viscoelasticity of maize starch pastes by adding sucrose at different stages. Food Hydrocolloids 19:777–784. https://doi.org/10.1016/j.foodhyd.2004.09.009

Hirashima M, Takahashi R, Nishinari K (2012) The gelatinization and retrogradation of cornstarch gels in the presence of citric acid. Food Hydrocolloids 27:390–393. https://doi.org/10.1016/j.foodhyd.2011.10.011

Hunter RJ (1998) Introduction to modern colloid science. Oxford University Press, Oxford, p 110

Hyun K, Wilhelm M, Klein CO, Cho KS, Nam JG, Ahn KH, Lee SJ, Ewoldt RH, McKinley GH (2011) A review of nonlinear oscillatory shear tests: Analysis and application of large amplitude oscillatory shear (LAOS). https://doi.org/10.1016/j.progpolymsci.2011.02.002

Ikeda S, Nishinari K (2001a) Solid-like mechanical behaviors of ovalbumin aqueous solutions. International Journal of Biological Macromolecules 28:315–320. https://doi.org/10.1016/S0141-8130(01)00128-3

Ikeda S, Nishinari K (2001b) Structural changes during heat-induced gelation of globular protein dispersions. Biopolymers 59:87–102. https://doi.org/10.1002/1097-0282(200108)59:2<87::AID-BIP1008>3.0.CO;2-H

Jaishankar A (2014) The linear and nonlinear rheology of multiscale complex fluids. (PhD thesis). MIT, USA. https://dspace.mit.edu/handle/1721.1/92159

Jaishankar A, McKinley GH (2012) Power-law rheology in the bulk and at the interface: quasi-properties and fractional constitutive equations. Physical and Engineering Sciences 469:1–21. https://doi.org/10.1098/rspa.2012.0284

Jaishankar A, McKinley GH (2014) A fractional KBKZ constitutive formulation for describing the nonlinear rheology of multi-scale complex fluids. Journal of Rheology 58:1751–1788. https://doi.org/10.1122/1.4892114

Jaishankar A, Wee M, Matia-Merino L, Goh KKT, McKinley GH (2015) Probing hydrogen bond interactions in a shear thickening polysaccharide using nonlinear shear and extensional rheology. Carbohydrate Polymers 123:136–145. https://doi.org/10.1016/j.carbpol.2015.01.006

Jang KJ, Hong YE, Moon Y, Jeon S, Angalet S, Kweon M (2018) Exploring the applicability of tamarind gum for making gluten-free rice bread. Food Science and Biotechnology 27:1639–1648. https://doi.org/10.1007/s10068-018-0416-z

Jensen S, Rolin C, Ipsen R (2010) Stabilisation of acidified skimmed milk with HM pectin. Food Hydrocolloids 24:291–299. https://doi.org/10.1016/j.foodhyd.2009.10.004

Kiani H, Mousavi ME, Razavi H, Morris ER (2010) Effect of Gellan, alone and in combination with high-methoxy pectin, on the structure and stability of doogh, a yogurt-based Iranian drink. Food Hydrocolloids 24:744–754. https://doi.org/10.1016/j.foodhyd.2010.03.016

Kita N, Senda M, Nagatsuka N, Nagao K (2009) Mechanical Properties and radical scavenging activity of unpolished rice noodles with added tamarind. Journal of Cookery Science of Japan 42:183–187. https://doi.org/10.11402/cookeryscience.42.183

Klinmalai P, Hagiwara T, Sakiyama T, Ratanasumawong S (2017) Chitosan effects on physical properties, texture, and microstructure of flat rice noodles. LWT - Food Science and Technology 76:117–123. https://doi.org/10.1016/j.lwt.2016.10.052

Kobayashi N, Kohyama K, Shiozawa K (2010) Fragmentation of a viscoelastic food by human mastication. Journal of the Physical Society of Japan 79:044801. https://doi.org/10.1143/JPSJ.79.044801

Koeller RC (1984) Applications of fractional calculus to the theory of viscoelasticity. Journal of Applied Mechanics 51:299–307. https://doi.org/10.1115/1.3167616

Kokelaar JJ, van Vliet T, Prins A (1996) Strain hardening properties and extensibility of flour and gluten doughs in relation to breadmaking performance. Journal of Cereal Science 24:199–214. https://doi.org/10.1006/jcrs.1996.0053

Krystyjan M, Sikora M, Adamczyk G, Tomasik P (2012) Caramel sauces thickened with combinations of potato starch and Xanthan Gum. Journal of Food Engineering 112:22–28. https://doi.org/10.1016/j.jfoodeng.2012.03.035

Lapasin R, Pricl S (1999) Rheology of industrial polysaccharides: theory and applications. Springer, New York

Larson RG (1999) The Structure and rheology of complex fluids. Oxford University Press, Oxford

Lazaridou A, Duta D, Papageorgiou M, Belc N, Biliaderis CG (2007) Effects of hydrocolloids on dough rheology and bread quality parameters in gluten-free formulations. Journal of Food Engineering 79:1033–1047. https://doi.org/10.1016/j.jfoodeng.2006.03.032

Lee HC, Brant DA (2002) Rheology of concentrated isotropic and anisotropic xanthan solutions. 2. A semiflexible wormlike intermediate molecular weight sample. Macromolecules 35:2223–2234. https://doi.org/10.1021/ma011527e

Li X, Fang Y, Zhang H, Nishinari K, Al-Assaf S, Phillips GO (2011) Rheological properties of gum arabic solution: from Newtonianism to thixotropy. Food Hydrocolloids 25:293–298. https://doi.org/10.1016/j.foodhyd.2010.06.006

Liang S, Li B, Ding Y, Xu BL, Chen J, Zhu B, Ma MH, Kennedy JF, Knill CJ (2011) Comparative investigation of the molecular interactions in konjac gum/hydrocolloid blends: concentration addition method (CAM) versus viscosity addition method (VAM). Carbohydrate Polymers 83:1062–1067. https://doi.org/10.1016/j.carbpol.2010.08.026

Lindstrom SB, Kodger TE, Sprakel J, Weitz DA (2012) Structures, stresses, and fluctuations in the delayed failure of colloidal gels. Soft Matter 8:3657–3664. https://doi.org/10.1039/C2SM06723D

Lynch KM, Coffey A, Arendt EK (2018) Exopolysaccharide producing lactic acid bacteria: their techno-functional role and potential application in gluten-free bread products. Food Research International 110:52–61. https://doi.org/10.1016/j.foodres.2017.03.012

Maeda H, Nakamura A (2021) Soluble soybean polysaccharide. In: Phillips GO, Williams PA (eds) Handbook of hyrocolloids, 3rd edn. Woodhead Publishing, Cambridge, pp 463–480. https://doi.org/10.1016/B978-0-12-820104-6.00025-5

Mewis J, Wagner NJ (2012) Colloidal suspension rheology. Cambridge University Press, Cambridge

Morimoto N, Tabara A, Seguchi M (2015) Effect of Xanthan Gum on improvement of bread height and specific volume upon baking with frozen and thawed dough. Food Science and Technology Research 21:309–316. https://doi.org/10.3136/fstr.21.309

Morris ER, Cutler AN, Ross-Murphy SB, Rees DA, Price J (1981) Concentration and shear rate dependence of viscosity in random coil polysaccharide solutions. Carbohydrate Polymers 1:5–21. https://doi.org/10.1016/0144-8617(81)90011-4

Mϕller PCF, Mewis J, Bonn D (2006) Yield stress and thixotropy: on the difficulty of measuring yield stresses in practice. Soft Matter 2:274–283. https://doi.org/10.1039/b517840a

Mϕller PCF, Fall A, Bonn D (2009) Origin of apparent viscosity in yield stress fluids below yielding. Europhysics Letters 87:38004. https://doi.org/10.1209/0295-5075/87/38004

Nakamura K, Shinoda E, Tokita M (2001) The influence of compression velocity on strength and structure for gellan gels. Food Hydrocolloids 15:247–252. https://doi.org/10.1016/S0268-005X(01)00021-2

Ng TSK, McKinley GH, Ewoldt RH (2011) Large amplitude oscillatory shear flow of gluten dough: a model power-law gel. Journal of Rheology 55:627–654. https://doi.org/10.1122/1.3570340

Nishinari K (1988) Food hydrocolloids in Japan. In: Phillips GO, Wedlock DJ, Williams PA (eds) Gums and stabilisers for the food industry, vol 4. IRL Press, Oxford, pp 373–390

Nishinari K (2004) Rheology, food texture and mastication. Journal of Texture Studies 35:113–124. https://doi.org/10.1111/j.1745-4603.2004.tb00828.x

Nishinari K, Fang Y (2018) Perception and measurement of food texture: solid foods. Journal of Texture Studies 49:160–201. https://doi.org/10.1111/jtxs.12327
Nishinari K, Horiuchi H, Ishida K, Ikeda K, Date E, Fukada E (1980) A new apparatus for rapid and easy measurement of dynamic viscoelasticity for gel-like foods. Nippon Shokuhin Kogyo Gakkaishi 27:227–233. https://doi.org/10.3136/nskkk1962.27.5_227
Nishinari K, Kohyama K, Williams PA, Phillips GO, Burchard W, Ogino K (1991) Solution properties of pullulan. Macromolecules 24:5590–5593
Nishinari K, Takemasa M, Zhang H, Takahashi R (2007) Storage plant polysaccharides: xyloglucans, galactomannans, glucomannan. In: Kamerling JP (ed) Comprehensive glycoscience, vol 2. Elsevier, London, pp 614–652
Nishinari K, Takemasa M, Su L, Michiwaki Y, Mizunuma H, Ogoshi H (2011) Effect of shear thinning on aspiration - toward making solutions for judging the risk of aspiration. Food Hydrocolloids 25:1737–1743. https://doi.org/10.1016/j.foodhyd.2011.03.016
Nishinari K, Takemasa M, Brenner T, Su L, Fang Y, Hirashima M, Yoshimura M, Nitta Y, Moritaka H, Tomczynska-Mleko M, Mleko S, Michiwaki Y (2016) The food colloid principle in the design of elderly food. Journal of Texture Studies 47:284–312. https://doi.org/10.1111/jtxs.12201
Nishinari K, Turcanu M, Nakauma M, Fang Y (2019) Role of fluid cohesiveness in safe swallowing. NPJ Science of Food 3:5. https://doi.org/10.1038/s41538-019-0038-8
Nitta Y, Yoshimura Y, Ganeko N, Ito H, Okushima N, Kitagawa M, Nishinari K (2018) Utilization of Ca^{2+}-induced setting of alginate or low methoxyl pectin for noodle production from japonica rice. LWT - Food Science and Technology 97:362–369. https://doi.org/10.1016/j.lwt.2018.07.027
Nussinovitch A, Hirashima M (2019) More cooking innovations –novel hydrocolloids for special dishes. CRC Press, Cleveland
Padalino L, Conte A, Del Nobile MA (2016) Overview on the general approaches to improve gluten-free pasta and bread. Foods 5:87. https://doi.org/10.3390/foods5040087
Pahwa A, Kaur A, Puri R (2016) Influence of hydrocolloids on the quality of major flat breads: a review. Journal of Food Processing 2016:8750258. https://doi.org/10.1155/2016/8750258
Parker A, Boulenguer P, Kravtchenko TP (1994) Effect of the addition of high methoxy pectin on the rheology and colloidal stability of acid milk drinks. In: Nishinari K, Doi E (eds) Food hydrocolloids: structures, properties, and functions. Springer, Boston, pp 307–312. https://doi.org/10.1007/978-1-4615-2486-1_48
Patel AR, Schatteman D, De Vos WH, Lesaffer A, Dewettinck K (2013) Preparation and rheological characterization of shellac oleogels and oleogel-based emulsions. Journal of Colloid and Interface Science 411:114–121. https://doi.org/10.1016/j.jcis.2013.08.039
Paximada P, Koutinas A, Scholten E, Mandala IG (2016) Effect of bacterial cellulose addition on physical properties of WPI emulsions. comparison with common thickeners. Food Hydrocolloids 54:245–254. https://doi.org/10.1016/j.foodhyd.2015.10.014
Pellicer J, Delegido J, Dolz J, Dolz M, Hernández MJ, Herráez MJ (2000) Influence of shear rate and concentration ratio on viscous synergism. application to xanthan-locust bean gum-NaCMC mixtures. Food Science and Technology International 6:415–423. https://doi.org/10.1177/108201320000600508
Peyron MA, Woda A (2016) An update about artificial mastication. Current Opinion in Food Science 9:21–28. https://doi.org/10.1016/j.cofs.2016.03.006
Picout DR, Ross-Murphy SB (2007) On the Mark–Houwink parameters for galactomannans. Carbohydrate Polymers 70:145–148
Picout DR, Ross-Murphy SB, Errington N, Harding SE (2001) Pressure cell assisted solution characterization of polysaccharides I: guar gum. Biomacromolecules 2:1301–1309
Pongsawatmanit R, Temsiripong T, Ikeda S, Nishinari K (2006) Influence of tamarind seed xyloglucan on rheological properties and thermal stability of tapioca starch. Journal of Food Engineering 77:41–50. https://doi.org/10.1016/j.jfoodeng.2005.06.017
Powel PC (1994) Engineering with fibre-polymer laminates. Springer, New York, p 68

Rai S, Kaur A, Chopra CS (2018) Gluten-free products for celiac susceptible people. Frontiers in Nutrition 5:116. https://doi.org/10.3389/fnut.2018.00116

Renard D, Axelos MAV, Boue F, Lefebvre J (1996) Small Angle neutron scattering and viscoelasticity study of the colloidal structure of aqueous solutions and gels of a globular protein. Journal de Chimie Physique et de Physico-Chimie Biologique 93:998–1015. https://doi.org/10.1051/jcp/1996930998

Reiner M (1971) Advanced rheology. Lewis, London

Richardson RK, Ross-Murphy SB (1987a) Non-linear viscoelasticity of polysaccharide solutions. 1: guar galactomannan solutions. International Journal of Biological Macromolecules 9:250–256. https://doi.org/10.1016/0141-8130(87)90062-6

Richardson RK, Ross-Murphy SB (1987b) Non-linear viscoelasticity of polysaccharide solutions. 2: Xanthan polysaccharide solutions. International Journal of Biological Macromolecules 9:257–264. https://doi.org/10.1016/0141-8130(87)90063-8

Risica D, Barbetta A, Vischetti L, Cametti C, Dentini M (2010) Rheological properties of guar and its methyl, hydroxypropyl and hydroxylpropyl-methyl derivatives in semidilute and concentrated aqueous solutions. Polymer 51:1972–1982. https://doi.org/10.1016/j.polymer.2010.02.041

Rogosin S, Mainardi F (2014) George William Scott Blair -- The Pioneer of Fractional Calculus in Rheology. arXiv:1404.3295. https://doi.org/10.1685/journal.caim.481

Rühmkorf C, Rübsam H, Becker T, Bork C, Voiges K, Mischnick P, Brandt MJ, Vogel RF (2012) Effect of structurally different microbial homoexopolysaccharides on the quality of gluten-free bread. European Food Research and Technology 235:139–146. https://doi.org/10.1007/s00217-012-1746-3

Sanderson GR (1981) Applications of Xanthan Gum. The British Polymer Journal 13:71–75. https://doi.org/10.1002/pi.4980130207

Sato T, Norisuye T, Fujita H (1984) Double-stranded helix of xanthan: dimensional and hydrodynamic properties in 0.1 M aqueous sodium chloride. Macromolecules 17:2696–2700

Scott Blair GW (1947) The role of psychophysics in rheology. Journal of Colloid Science 2:21–31. https://doi.org/10.1016/0095-8522(47)90007-X

Scott Blair GW (1969) Elementary rheology. Academic, London

Shao P, Qin M, Han L, Peilong Sun P (2014) Rheology and characteristics of sulfated polysaccharides from chlorophytan seaweeds ulva fasciata. Carbohydrate Polymers 113:365–372. https://doi.org/10.1016/j.carbpol.2014.07.008

Shi Z, Zhang Y, Phillips GO, Yang G (2014) Utilization of bacterial cellulose in food. Food Hydrocolloids 35:539–545. https://doi.org/10.1016/j.foodhyd.2013.07.012

Shingel KI (2004) Current knowledge on biosynthesis, biological activity, and chemical modification of the exopolysaccharide pullulan. Carbohydrate Research 339:447–460

Silva E, Birkenhake M, Scholten E, Sagis LMC, van der Linden E (2013) Controlling rheology and structure of sweet potato starch noodles with high broccoli powder content by hydrocolloids. Food Hydrocolloids 30:42–52. https://doi.org/10.1016/j.foodhyd.2012.05.002

Smidsrød O, Haug A (1971) Estimation of the relative stiffness of the molecular chain in polyelectrolytes from measurements of viscosity at different ionic strengths. Biopolymers 10:1213–1227. https://doi.org/10.1002/bip.360100711

Sprakel J, Lindstrom SB, Kodger TE, Weitz DA (2011) Stress enhancement in the delayed yielding of colloidal gels. Physical Review Letters 106:248303. https://doi.org/10.1103/PhysRevLett.106.248303

Steele CM, Alsanei WA, Ayanikalath S, Barbon CE, Chen J, Cichero JA, Coutts K, Dantas RO, Duivestein J, Giosa L, Hanson B, Lam P, Lecko C, Leigh C, Nagy A, Namasivayam AM, Nascimento WV, Odendaal I, Smith CH, Wang H (2015) The influence of food texture and liquid consistency modification on swallowing physiology and function: a systematic review. Dysphagia 30:2–26. https://doi.org/10.1007/s00455-014-9578-x

Stokes JR, Telford JH (2004) Measuring the yield behaviour of structured fluids. Journal of Non-Newtonian Fluid Mechanics 124:137–146. https://doi.org/10.1016/j.jnnfm.2004.09.001

Suchkov VV, Popello IA, Grinberg VY, Tolstoguzov VB (1997) Shear effects on phase behaviour of the legumin-salt-water system. Modelling protein recovery. Food Hydrocolloids 11:135–144. https://doi.org/10.1016/S0268-005X(97)80021-5

Sun ZH, Wang W, Feng ZL (1992) Criterion of polymer– polymer miscibility determined by viscometry. European Polymer Journal 28:1259–1261. https://doi.org/10.1016/0014-3057(92)90215-N

Sworn G (2021) Xanthan gum. Woodhead Publishing pp, Cambridge, pp 833–853. https://doi.org/10.1016/B978-0-12-820104-6.00004-8

Turcanu M, Siegert N, Secouard S, Brito-de la Fuente E, Balan C, Gallegos C (2018) An alternative elongational method to study the effect of saliva on thickened fluids for dysphagia nutritional support. Journal of Food Engineering 228:79–83. https://doi.org/10.1016/j.jfoodeng.2018.02.015

van Riemsdijk LE, van der Goot AJ, Hamer RJ (2011) The use of whey protein particles in gluten-free bread production, the effect of particle stability. Food Hydrocolloids 25:1744–1750. https://doi.org/10.1016/j.foodhyd.2011.03.017

Wagner CE, Barbati AC, Engmann J, Burbidge AS, McKinley GH (2016) Apparent shear thickening at low shear rates in polymer solutions can be an artifact of non-equilibration. Applied Rheology 26:54091. https://doi.org/10.3933/ApplRheol-26-54091

Wagner CE, Barbati AC, Engman J, Burbidge AS, McKinley GH (2017) Quantifying the consistency and rheology of liquid foods using fractional calculus. Food Hydrocolloids 69:242–254. https://doi.org/10.1016/j.foodhyd.2017.01.036

Waigh TA (2016) Advances in the microrheology of complex fluids. Reports on Progress in Physics 79:074601. https://doi.org/10.1088/0034-4885/79/7/074601

Wientjes RHW, Duits MHG, Jongschaap RJJ, Mellema J (2000) Linear rheology of guar gum solutions. Macromolecules 33:9594–9605. https://doi.org/10.1021/ma001065p

Wu M, Qu J, Tian X, Zhao X, Shen Y, Shi Z, Chen P, Li G, Ma T (2019) Tailor-made polysaccharides containing uniformly distributed repeating units based on the xanthan gum skeleton. International Journal of Biological Macromolecules 131:646–653. https://doi.org/10.1016/j.ijbiomac.2019.03.130

Wyatt NB, Gunther CM, Liberatore MW (2011) Increasing viscosity in entangled polyelectrolyte solutions by the addition of salt. Polymer 52:2437–2444. https://doi.org/10.1016/j.polymer.2011.03.053

Yalpani M, Hall LD, Tung MA, Brooks DE (1983) Unusual rheology of a branched, water- soluble chitosan derivative. Nature 302:812–814. https://doi.org/10.1038/302812a0

Yang N, Lv R, Jia J, Nishinari K, Fang Y (2017) Application of microrheology in food science. Annual Review of Food Science and Technology 8:23.1–23.29. https://doi.org/10.1146/annurev-food-030216-025859

Yang X, Gong T, Lu YH, Li A, Sun L, Guo Y (2020) Compatibility of sodium alginate and konjac glucomannan and their applications in fabricating low-fat mayonnaise-like emulsion gels. Carbohydrate Polymers 229:115468. https://doi.org/10.1016/j.carbpol.2019.115468

Yazar G, Duvarci O, Tavman S, Kokini JL (2017a) LAOS behavior of the two main gluten fractions: gliadin and glutenin. Journal of Cereal Science 77:201–210. https://doi.org/10.1016/j.jcs.2017.08.014

Yazar G, Duvarci O, Tavman S, Kokini JL (2017b) Non-linear rheological behavior of gluten-free flour doughs and correlations of laos parameters with gluten-free bread properties. Journal of Cereal Science 74:28–36. https://doi.org/10.1016/j.jcs.2017.01.008

Yeung YK, Lee YK, Chang YH (2019) Physicochemical, microbial, and rheological properties of yogurt substituted with pectic polysaccharide extracted from *Ulmus davidiana*. Journal of Food Process and Preservation 43:e13907. https://doi.org/10.1111/jfpp.13907

Zhang L, Zhou F (2006) Synergistic viscosity characteristics of aqueous mixed solutions of hydroxypropyl- and carboxymethyl hydroxypropyl-substituted guar gums. Colloids and Surfaces A 279:34–39. https://doi.org/10.1016/j.colsurfa.2005.12.030

Zhang F, Luan T, Kang D, Jin Q, Zhang H, Yadav MP (2015) Viscosifying properties of corn fiber gum with various polysaccharides. Food Hydrocolloids 43:218–227. https://doi.org/10.1016/j.foodhyd.2014.05.018

Zhao M, Cui N, Qu F, Huang X, Yang H, Nie S, Zha X, Cui SW, Nishinari K, Phillips GO, Fang Y (2017) Novel nano-particulated exopolysaccharide produced by *Klebsiella* sp. PHRC1.001. Carbohydrate Polymers 171:252–258. https://doi.org/10.1016/j.carbpol.2017.05.015